Building and Environment 299 (2026) 114692

Contents lists available at ScienceDirect

Building and Environment

journal homepage: www.elsevier.com/locate/buildenv

Tracking PM_{10} composition and source assignment in classrooms and schoolyard: A case study near an industrial estate

Isabella Charres [a,*], Yago Cipoli [a], Estela D. Vicente [a], Leonardo Furst [a], Teresa Nunes [a], Ana M. Sánchez de la Campa [b,c], Manuel Feliciano [d], Célia Alves [a]

[a] Centre for Environmental and Marine Studies (CESAM), Department of Environment, University of Aveiro, 3810-193, Aveiro, Portugal
[b] Center for Research in Sustainable Chemistry-CIQSO, Associate Unit CSIC-University of Huelva "Atmospheric Pollution", Campus El Carmen s/n, 21071 Huelva, Spain
[c] Department of Earth Sciences, Faculty of Experimental Sciences, University of Huelva, Huelva, 21007, Spain
[d] CIMO, LA SusTEC, Instituto Politécnico de Bragança, Campus de Santa Apolónia, 5300-253 Bragança, Portugal

ARTICLE INFO

Keywords:
Pm10
School environment
Mass closure
Factor analysis
Source identification

ABSTRACT

Schools are essential environments where people spend a significant portion of their early lives. Air quality in schools is shaped by various factors, including location, climate, and surrounding activities. Additionally, both indoor and outdoor sources can release chemicals into the air, potentially exposing pupils and staff to harmful conditions. This work characterised the chemical composition and potential sources of particulate matter (PM_{10}) in a school, with different educational levels, located near an industrial estate in Portugal. PM_{10} daily samples were measured in classrooms and the schoolyard in two seasons. Samples were analysed by chromatography, inductively coupled plasma-mass spectrometry and thermo-optical transmittance techniques. Ancillary tools, such as factor analysis, multiple linear regression, meteorological analysis and air mass backward trajectories were applied to determine source contributions. Mass closure analysis revealed that organic matter accounted for ~39% of the PM_{10} mass in both seasons. Six sources were identified as contributors to PM_{10} in both the classrooms and the schoolyard. Common sources included biomass burning (18% and 28%), mineral dust (28% and 7.1%), sea salt (16% and 20%), and traffic (1.4% and 1.8%), for indoor and outdoor environments, respectively. In the classrooms, resuspension of calcium was a major contributor to PM_{10}, whereas in the schoolyard, secondary aerosol formation played a significant role.

1. Introduction

Between 2000 and 2017, the 27 EU member states and the United Kingdom (formerly the EU-28) achieved significant reductions in air pollutant emissions, including sulphur oxides (80%), nitrogen oxides (46%), non-methane volatile organic compound (44%), ammonium (10%), carbon monoxide (49%), and particulate matter with a diameter lower than 2.5 μm ($PM_{2.5}$, 31%), and 10 μm (PM_{10}, 29%), reflecting the effectiveness of air pollution control strategies [1]. Such reductions in PM are critical for schools, as indoor PM levels are partially dependent on ambient air [2–4], declining outdoor concentrations help reduce the baseline for indoor environments. However, decreasing outdoor levels does not guarantee a proportional drop indoors. Research shows that other factors, such as human activity, school supplies [5,6] and ventilation systems [2–4,7] play an important role in indoor PM_{10} concentrations.

Research across European schools shows a significant downward trend in PM_{10} concentrations. In 2013, during teaching hours in Wroclaw, the median indoor PM_{10} concentration reached 110 μg m^{-3} in winter, nearly double the outdoor levels recorded at the time [8]. In Porto between 2011 and 2013, the indoor median PM_{10} level of 127 μg m^{-3} was significantly higher than outdoor levels (75 μg m^{-3}) [6]. Most recent studies indicate a dramatic reduction in PM_{10} levels. In Gothenburg primary schools, the median PM_{10} concentration during occupied hours was found to be just 21 μg m^{-3} [7], and data from Swiss primary schools shows some of the lowest recorded levels. Median PM_{10} levels during school hours dropping 4 μg m^{-3} against an outdoor of 10 μg m^{-3} [3].

Despite overall reductions in PM_{10} in schools, concentrations remain consistently higher during school hours than during unoccupied periods [9,10]. In London, for example, average PM_{10} levels were approximately 130% and 150% higher during high and low occupancy hours compared

* Corresponding author.
E-mail address: isabellacharres@ua.pt (I. Charres).

https://doi.org/10.1016/j.buildenv.2026.114692
Received 31 January 2026; Received in revised form 22 April 2026; Accepted 2 May 2026
Available online 2 May 2026

to when classrooms were empty [10]. The health implications are documented across diverse environments. In Italy, PM_{10} exposure near industrial cement plants was linked to a 2.5% increase in school absenteeism [11]. Conversely, in urban Beijing, PM_{10} exposure during school hours was directly associated with over 7000 cases of wheezing and coughing among primary students [12]. These findings underscore that, due to the unique variables of each school, individualised assessments are essential to ensure that PM_{10} levels do not represent a risk for schoolchildren.

While previous research has studied and characterised PM in Portuguese urban and rural schools [13,14], industrial areas remain under-examined. This study addresses this gap by assessing PM_{10} concentrations in an institution near one of the largest industrial estates in the country, in an area defined by a complex mix of potential sources, moving beyond the typical traffic-dominated urban or rural profiles. Thus, the overarching aim of this paper was to provide a comprehensive snapshot of air quality within Portuguese school environments, based on PM_{10} samples collected over two seasons. To ensure data collection within the available research budget and logistic constraints, the study focused on the winter and spring seasons, following the specific goals: (i) characterising the chemical composition of PM_{10} both inside and outside classrooms; (ii) identifying and quantifying the main sources contributing to PM_{10}; (iii) and assessing the influence of outdoor PM_{10} on indoor air quality. We hypothesise that concentrations of PM_{10} in classrooms are higher compared to concentrations measured in the schoolyard during both winter and spring, despite the general downtrend in ambient PM_{10} concentrations in Portugal [15]. This study builds on previous research at the same school, which characterised ventilation conditions [16]. That study found that classrooms were insufficiently ventilated; CO_2 concentrations frequently exceeded 1000 ppm during occupancy, and air change rates ranged from 0.32 to 1.56 h^{-1} across seasons. Furthermore, ventilation rates failed to meet American Society of Heating, Refrigerating and Air-Conditioning Engineers standards, particularly in winter when windows remained closed. These conditions suggest that while outdoor PM_{10} can infiltrate the building, it likely accumulates indoors due to poor ventilation efficiency.

2. Methodology

2.1. Study area

The district of Aveiro (northern Portugal), where the Estarreja school is located, has a Mediterranean climate and is classified, according to the Köppen system, as a humid temperate climate with mild, dry summers (Csb) [17]. The average annual temperature is approximately 15.8 °C. The warmest months are typically July, August, and September, while the highest levels of precipitation occur during the winter months, particularly in October, November, and January [18]. Low temperatures and weak winds facilitate stable boundary layer conditions, promoting PM_{10} accumulation, while rain and stronger winds can reduce PM_{10} levels, especially in urban areas [19]. Because these meteorological parameters influence PM_{10} concentrations, a snapshot of Estarreja's weather conditions during the sampling period is provided in the Supplementary Material (**Fig. S1**).

The school is located near a railway and streets with minimal vehicle traffic. Portuguese basic education is divided into three stages: the 1st cycle (1st to 4th grades, ages 6–9), the 2nd cycle (5th and 6th grades, ages 10–11), and the 3rd cycle (7th to 9th grades, ages 12–14). The school involved in this study comprises four main buildings, each one dedicated to a different educational level: 1) Building D - preschool; 2)

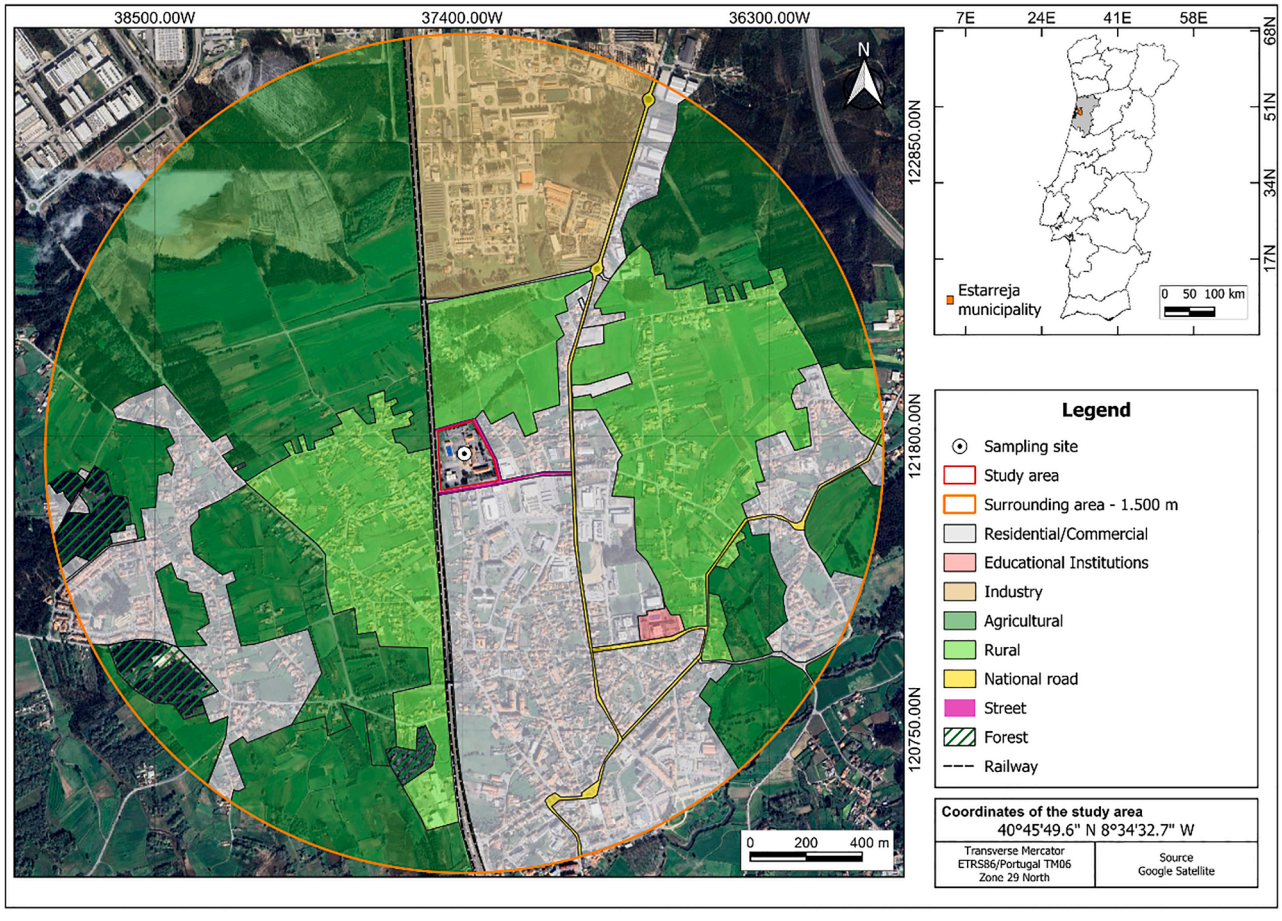

Fig. 1. Location of the sampling site.

Building B - 1st cycle; and 3) Buildings A and C - 2nd cycle. The monitoring locations and the school facilities are described in detail by Charres et al. [16]. The school has approximately 700 students aged between 3 and 12 years. In general, pupils attend school from 08:00 to 16:00.

As displays in Fig. 1, the school is located within a 1.5 km radius of a variety of land uses, ranging from residential neighbourhoods to areas with industrial activity in the north. Central to this landscape is the Estarreja Chemical Estate (ECE), one of the main chemical industry hubs in Portugal, with approximately 70% of the population living in its vicinity [20]. The ECE facilitates the production of both organic and inorganic chemicals such as aniline, chlorine, and its derivatives. Historically, industrial activity was the dominant source of pollution of PM_{10} in Estarreja, responsible for 95% of PM_{10} emissions in 2008 [21]. However, air quality improved markedly between 2000 and 2009. Specifically, from 2005 onwards, a sharp downward trend was recorded, median concentrations of PM_{10} and $PM_{2.5}$ dropped by nearly 50% (to 13 and 20 μg m^{-3}, respectively) by 2009 [21].

2.2. Data acquisition and study design

One classroom was selected from each of the four buildings to represent the educational levels offered at the school and the varying ages of the children (Table 1). Classrooms were selected based on two primary criteria: obtaining teacher authorisation and the availability of sufficient space to install equipment without disrupting regular class activities. The classrooms have white-painted concrete walls, wooden doors, whiteboards with markers, and rely primarily on natural ventilation. Prior to sampling, quartz fibre filters (15 cm diameter) were baked for 6 h at 500 °C to remove organic contaminants. PM_{10} sampling was carried out simultaneously indoors and outdoors, using two high-volume samplers at an airflow rate of 500 L min^{-1} (HVS, Model CAV-A/MSb, MCV S.A). Temporal resolution was 23.5 h between Monday and Thursday but decreased to 22 h on Fridays due to logistical constraints, including instrument transfer and earlier school closure. Field researchers coordinated filter changes at both locations to ensure that the sampling intervals differed as little as possible. Each campaign ran for four weeks from November - December 2022 (winter) and from April - May 2023 (spring). Sampling yielded 18 indoor and 17 outdoor sets in winter, followed by 17 indoor and 18 outdoor sets in spring. Following collection, filters were folded in half, face to face, wrapped in pre-calcined aluminium foil, stored in zip-lock bags, and transported to the laboratory, where they were frozen at −18 °C until gravimetric determination. The filters were only defrosted immediately prior to specific chemical analyses to maintain sample integrity.

For indoor sampling, the inlet was positioned at a height of 1.2 m above the floor, maintaining a minimum distance of 1 m from doors, windows, and walls. Simultaneously, outdoor sampling was conducted using a second high-volume sampler and a weather station. Meteorological data such as precipitation, temperature, wind speed and direction, among other parameters, was collected using a Davis Vantage Pro2 weather station, which recorded data every 10 min throughout both sampling campaigns. These instruments were positioned at ground level within a restricted area of the schoolyard to ensure secure, unsupervised data collection. The anemometers, wind vanes and the rain gauge were placed at height of 2 m above the surface.

Table 1
Description of sampling collection.

Locations	Measurement in winter	Measurement in spring
Nursery room (building D) and the schoolyard	Nov. 13–18, 2022	April 16–21, 2023
1st cycle room (building B) and the schoolyard	Nov. 20–25, 2022	April 23–28, 2023
2nd cycle room (building C) and the schoolyard	Nov. 27 - Dec. 02, 2022	May 01 - 05, 2023
2nd cycle room (building A) and the schoolyard	Dec. 04 - 09, 2022	May 07 – 12, 2023

2.3. Analytical techniques

Once the concentration of PM_{10} was calculated, the filters were cut into pieces of different sizes according to the laboratorial procedures to be applied. For determination of the carbonaceous content, a portion of each filter, consistent of two 11 mm diameter circle, was removed and analysed in a thermo-optical equipment, where organic carbon (OC) is volatilised from the sample in a non-oxidising N_2 atmosphere, while elemental carbon (EC) requires an oxidising atmosphere to volatilise (4% O_2). The released carbonaceous fractions are converted to CO_2, which is quantified in a non-dispersive infrared analyser (LI-COR Biosciences, model LI-6262). During heating in a non-oxidising atmosphere, a portion of the OC is pyrolyzed (PC) and quantified as EC. The separation of OC and EC is achieved by heating the sample initially in an inert atmosphere to volatilise the OC fraction, in accordance with the thermal temperature program developed as part of the European Supersites for Atmospheric Aerosol Research (EUSAAR-2) [22]. After, the remaining material is then sequentially volatilised or combusted under an oxygen-containing gas flow. To minimise interference between PC and EC, the degree of filter blackening is continuously monitored by employing a laser and photodetector to measure light transmittance. More details about the technique can be found in the Supplementary Material.

For ion analyses, two 19 mm diameter filter portions of each sample were leached in 4 mL Milli-Q water under ultrasonic agitation for 30 min. The extracts were divided into three aliquots: the first for the determination of cations, the second for anions, and the third for measuring carbohydrates. Cations (ammonium, NH_4^+; sodium, Na^+; potassium, K^+; calcium, Ca^{2+}; magnesium, Mg^{2+} and lithium, Li^+) were analysed using a Dionex DX-100 chromatograph. Anions (chloride, Cl^-; nitrate, NO_3^-, sulphate; SO_4^{2-}; fluoride, F^-; nitrite, NO_2^-; phosphate, PO_4^{3-} and bromide, Br^-) were analysed using a Shimadzu CDD-6A detector. For both solutions, a flow rate of 2 mL min^{-1} was used. System control and data analysis were managed using Chromeleon software.

Carbohydrates were quantified using high-performance anion exchange chromatography coupled with pulsed amperometric detection (HPAE-PAD). Sugars, anhydrosugars, and sugar alcohols were separated using a Carbopac PA-1 analytical column. System control and data analysis were managed using Chromeleon software. Quantification of the carbohydrates was achieved using external calibration curves prepared from solid standards from Sigma-Aldrich diluted in Milli-Q ultrapure water.

Finally, a portion of each filter (14.1 cm^{-2}) was extracted under acid digestion for the identification of major and trace elements using Inductively Coupled Plasma (ICP) mass spectroscopy (-MS) and optical emission spectroscopy (-OES), respectively, following the methodology described by Millán-Martínez et al. [23].

Details regarding chemical analysis quality assurance and quality control are provided on page 3 of the **Supplementary Material**.

2.4. Data processing

2.4.1. PM_{10} mass closure

This article aims to examine the general trends in PM_{10} behaviour across two school environments (classrooms and schoolyard). The reconstruction of PM_{10} mass has been summarised by ambient setting (indoor and outdoor), with the species grouped into categories according to their sources and chemical nature, as follows: organic matter (OM), elemental carbon (EC), Secondary Inorganic Aerosol (SIA), sea salt, mineral dust (MD) and trace elements. A simple conversion of OC to organic matter (OM) was performed using a factor of 1.8. This value is within the range normally used for urban aerosols [24]. For the other

groups, the species and equations considered in each category are the same as those described by Cipoli et al. [25] in the methodology and supplementary material.

2.4.2. Contribution of anthropogenic sources

To assess the contribution of anthropogenic sources to the concentration of a specific element in airborne PM_{10}, enrichment factors (EFs) were calculated using aluminium (Al) as the reference element using the equation described by Cipoli et al. [25]. These calculations were based on the average chemical composition of the upper continental crust as outlined by Wedepohl [79]. EFs greater than 10 suggest that the element primarily originates from anthropogenic sources, while values below 10 indicate that the element is predominantly of crustal origin.

2.4.3. Source apportionment

Source apportionment techniques, including receptor models like Positive Matrix Factorisation (PMF), and Principal Component Analysis (PCA), are essential tools for identifying pollution sources and quantifying their contributions [27,28]. The efficacy of these models depends on the availability of large datasets, as higher temporal resolution generally improves model output [28]. PMF is a popular and advanced method that accounts for data uncertainty, while PCA is a common alternative, although it has been found to perform less accurately than PMF in comparative studies [27]. Despite these differences, the identification of the emission sources of PM_{10} at the school was based on PCA and Multiple Linear Regression (PCA-MLR). This was selected because it is a basic and common factorisation technique that could provide initial estimates of source contributions. For this, the complete dataset from the two seasons was separated into two groups. Firstly, species with >15% of their concentration values below the limits of detection (LOD) were not included in subsequent analyses. Secondly, as reported in many studies [29,30], data below the LOD were substituted with LOD/2. Thirdly, the assumptions for carrying out a PCA were verified applying Kaiser-Meyer-Olkin (KMO) and Bartlett's Sphericity tests to the two datasets. Both tests were used to assess the suitability of the data for PCA. KMO and Bartlett values were greater than 0.65 and less than 0.3, respectively, for the two data sets (indoor and outdoor).

PCA was applied to data collected in the schoolyard and classrooms following the procedure described by Karar and Gupta [26]. Species concentration was standardised using Z-score. The optimal number of components in each dataset was decided based on eigenvalues greater than or equal to 1, to provide information on the most significant species and reduce each dataset with minimal loss of original information. Like other studies [32] varimax rotation was used to better interpret the PCA results. After rotation, the component loading concentrations on each day were transformed into absolute principal component scores (APCS).

Finally, the APCS were used as independent variables and the PM_{10} concentration measured at the school as dependent variable to determine the coefficients that convert the APCS into PM_{10} factor contributions (in mass concentration, $\mu g\ m^{-3}$) for each sampling day. In addition, both the forward selection approach and the backward elimination method were applied to test the statistical significance of the APCSs. The percentage contribution of each component (source) to each model and for each sample was estimated by multiplying each regression coefficient by the APCS value divided by the PM_{10} concentration of the corresponding sample.

2.4.4. Backward air mass trajectories

Trajectory analysis may play a key role in determining the transport and fate of PM_{10} at the school, thereby enhancing confidence in identifying sources. Therefore, backward air mass trajectories were generated using HYSPLIT, accessed through the Real-time Environmental Applications and Display System on the NOAA website. HYSPLIT was configured to provide 120 h trajectories arriving at the school 500 m above the ground level, at 18:00 local time, with 4 h intervals. Additionally, to account for daily trajectories during the two sampling periods, a hierarchical cluster analysis was performed on the end points of the daily trajectories to group days with similar patterns.

3. Results and discussion

3.1. PM_{10} concentrations and mass closure

The daily PM_{10} concentrations ranged from 9.85 to 51.7 $\mu g\ m^{-3}$, with an average of 26.5 $\mu g\ m^{-3}$ for both fieldworks. In classrooms, PM_{10} concentrations were $24.0 \pm 8.62\ \mu g\ m^{-3}$ in winter and $26.5 \pm 7.84\ \mu g\ m^{-3}$ in spring (Fig. 2), with the highest value being recorded on a spring day characterised by high temperature (24 °C) and low humidity (49%). In contrast to indoor measurements, the PM_{10} concentration in the schoolyard was $27.3 \pm 9.09\ \mu g\ m^{-3}$, with higher mean values in winter ($29.4 \pm 12.0\ \mu g\ m^{-3}$) than in spring ($26.0 \pm 5.57\ \mu g\ m^{-3}$). In addition, wind speeds were generally lower in winter than in spring (**Fig. S2**). The highest concentration ($51.7\ \mu g\ m^{-3}$) was observed on a day with high humidity (82%) and low temperature (12 °C).

PM_{10} concentrations in the schoolyard are generally lower than those found in other schools in different parts of the world (Table 2). In Estarreja, the mean PM_{10} concentration in classrooms was 2.8 and 1.6 times lower than that found in a Polish school in winter and summer, respectively. The PM_{10} values observed in the two seasons in Estarreja are lower than those recorded in Korean classrooms, where some of which use air purifiers. In winter, PM_{10} levels were also up to 5.8 lower than those recorded in Porto classrooms a few years ago. However, the PM_{10} levels in classrooms of this study are up to 7 times higher than those to which Finnish students are exposed on a winter school day. Note that comparing PM_{10} concentrations across studies should be done cautiously, as differences in sampling times - class time versus 24-hour periods - can impact the results.

A good correlation was observed between the PM_{10} concentration measured by gravimetry and the concentration calculated through mass closure (**Fig. S2**). The total sum of the major compounds accounted for at least 66% of the PM_{10} mass indoors and 60% outdoors (Table 3). In the schoolyard samples, there were specific days when the mass reconstruction was lower than expected. These days coincided with the rainiest periods of winter sampling. However, other factors such as uncertainties in the analytical techniques and mass losses during filter handling may have also contributed to the lower PM_{10} mass reconstruction. Indoor samples generally showed higher mass contributions from some components compared to outdoor samples. Specifically, in both seasons, the main contributor to PM_{10} mass was OM. In winter, it was the dominant component, both indoors and outdoors. In spring, outdoor samples showed a higher contribution from MD and sea salt, while indoor samples exhibited a greater share from MD. These variations highlight the influence of point-specific factors, such as local pollution sources, school environmental conditions, and pupils' activities on PM_{10} mass composition throughout the study.

OC was more abundant in classrooms, with an average daily concentration of 5.53 $\mu g\ m^{-3}$, compared to 3.44 $\mu g\ m^{-3}$ outside. EC exhibited similar average values in both classrooms and the playground (Table 3). However, some differences were observed when analysing the OC/EC ratio for the two environments. The average OC/EC ratios were 3.83 and 9.85 in the schoolyard in winter and spring, respectively, while in the classrooms, the values were more than double those observed outdoors (8.73 and 26.4, respectively). Previous studies in school environments in Portugal reported OC/EC > 4 in classrooms in Aveiro Alves et al. [34] and 15 and 6.1 indoors and outdoors in Lisbon, respectively [35]. When comparing the ratios, some differences between the schools should be considered. Firstly, the sampling dates do not overlap with those in Estarreja. Secondly, the sampling in other Portuguese schools was carried out during occupancy hours. In Lisbon, the reported values represent the average of 5 primary schools, while in Aveiro, the value was obtained from a field sampling that lasted 3 months. Overall, the high OC/EC values in classrooms of this study may

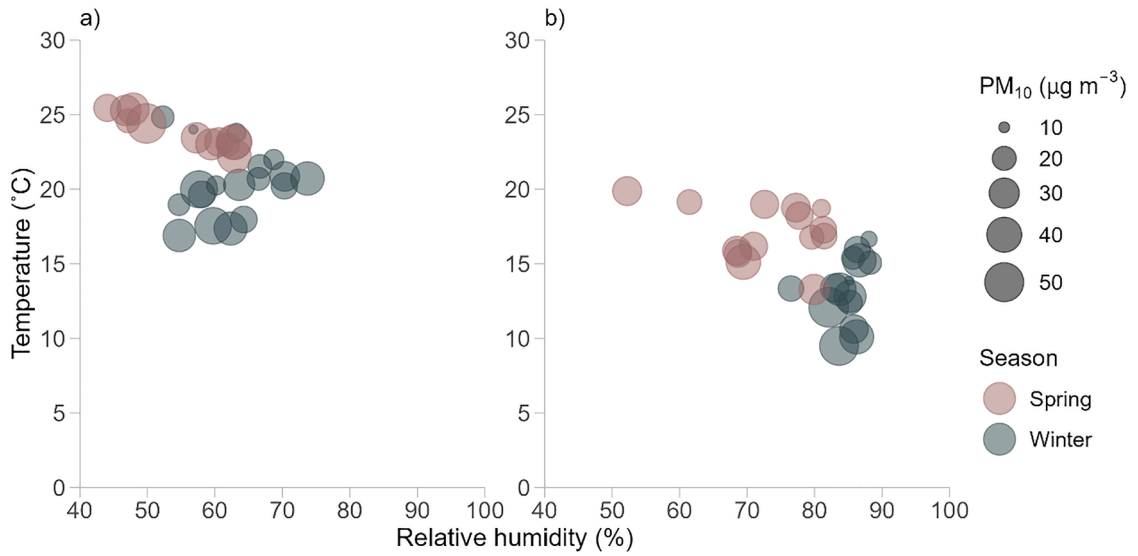

Fig. 2. PM_{10} concentrations as a function of temperature and relative humidity in (a) classrooms, and (b) schoolyard.

Table 2
Mean concentrations of PM_{10} (µg m^{-3}) found in school environments in different countries.

Study and location	Indoor	Outdoor	Season	Sampling duration and instrumentation
This study Estarreja, Portugal	24.0 ± 8.62 26.5 ± 7.84	29.4 ± 12.0 25.6 ± 5.57	Early winter Spring	23.2 h (5 days / week) Gravimetric technique
Han et al. [33] Seoul, Korea	45.5 ± 4.1 109.1 ± 9.6	74.1 ± 10.6	Early winter 4 classrooms, equipped with one air cleaner 4 classrooms, natural ventilation	Class time (5 days /6 h) Optical measurements
Madureira et al. [6] (Porto, Portugal)	139 ± 49	88 ± 64	Winter 57 classrooms, natural ventilation	Class time (5 days / 8 h) Optical measurements
Zwoździak et al. [8] (Wroclaw, Poland)	68.5 ± 21.8 43.1 ± 17.9	56.8 ± 17.3 24.7 ± 10.5	Winter Summer 1 classroom, natural ventilation	24 h Harvard cascade impactors
Vornanen-Winqvist et al. [31] (Helsinki, Finland)	1.8–3.4	Not measured	Winter 4 classrooms, mechanical supply and extract ventilation	Working hours (9 h) MIE pDR-1500 nephelometer

indicate the influence of primary sources and the formation of secondary organic aerosols, as observed in previous research Alves et al. [35].

SIA concentrations were higher in spring than in winter (Table 3), likely due to increased sunlight and temperature, which promote photochemical processes and lead to the increased formation of both nitrate and sulphate [36]. $nssSO_4^{2-}$ accounted for ~55% and ~74% of total SO_4^{2-} in winter and spring, respectively, pointing to anthropogenic activities as the main sources of SO_4^{2-} at the school. Positive and statistically significant correlations between NH_4^+, NO_3^-, K^+ and $nssSO_4^{2-}$ indicate that PM_{10} in winter is influenced by combustion sources (**Fig. S3**), principally biomass burning for heating. In the cold season,

Table 3
Chemical mass closure of PM_{10} collected in classrooms and the schoolyard. The values correspond to the reconstructed concentration (µg m^{-3}). The standard deviation is presented in brackets (±).

	Winter		Spring	
Components	Indoor	Outdoor	Indoor	Outdoor
OM	11.9 (6.96)	10.4 (9.51)	7.90 (2.55)	3.18 (2.55)
EC	1.36 (1.24)	1.70 (1.68)	0.31 (0.22)	0.39 (0.38)
SIA	1.09 (0.79)	1.81 (1.17)	1.99 (0.64)	2.98 (0.96)
Sea salt	2.64 (2.37)	3.48 (2.52)	2.26 (1.62)	4.04 (2.42)
Mineral dust	2.56 (1.25)	1.80 (1.19)	4.89 (3.67)	4.21 (3.07)
Trace elements	0.19 (0.17)	0.36 (0.31)	0.17 (0.10)	0.22 (0.13)
Other	4.21 (4.14)	9.80 (4.50)	8.99 (3.84)	10.5 (3.54)
PM_{10} reconstructed	19.7 (9.37)	19.6 (12.5)	17.5 (5.22)	15.1 (5.70)

the positive correlation between $nssSO_4^{2-}$ and NO_3^- ($r^2 = 0.84$) likely reflects the emission of precursor gases from common sources. The positive correlation between NH_4^+ and $nssSO_4^{2-}$ ($r^2 = 0.74$) suggests the formation of ammonium sulphate. Unlike in winter, only one positive correlation was observed in spring (**Fig. S3**): NH_4^+ versus $nssSO_4^{2-}$ ($r^2 = 0.89$). The differences in correlations between winter and spring could be explained by several factors related to seasonal variations in atmospheric conditions, sources of pollution, and chemical processes.

The contribution of sea salt to the PM_{10} mass is most pronounced in the measurements taken in the schoolyard, reaching its peak during the winter weeks. Studies conducted in Portuguese coastal cities have shown that sea salt levels are significantly higher in winter than in summer, mainly due to increased wave energy and stronger oceanic winds during the colder season [37]. In this study, good correlations were found between key sea salt tracers, both indoors and outdoors, in both seasons. Specifically, Cl^- and Na^+ displayed a strong correlation with an $r^2 > 0.84$, while Cl^- and Mg^{2+} also exhibited a strong correlation with an r^2 exceeding 0.86. However, it is possible that these elements may originate from sources other than sea salt (**Fig. S4**), with cleaning products used in the classrooms potentially influencing the concentrations of Cl^- and Na^+. To explore this further, the Cl^-/Na^+ and Mg^{2+}/Na^+ ratios in the schoolyard were calculated to assess whether they aligned with the values found in seawater, helping to determine whether Na^+ and Cl^- could be classified as either marine or non-marine in origin.

The Mg^{2+}/Na^+ ratios in all filters were found to be very close (mean: 0.13 ± 0.01) to the expected value in seawater (0.12), indicating that Na^+ in the schoolyard was primarily of marine origin. Some filters showed Cl^-/Na^+ ratios below 1.81 (the seawater ratio), suggesting that

anthropogenic sources contributing to chloride (e.g., emissions from PVC manufacturing in the industrial estate, or cleaning products) are less active in the period in question and/or that chloride has volatilised. In fact, Cl^- can easily volatilise, especially in warmer conditions or in the presence of certain chemicals (e.g., H_2SO_4 and HNO_3), which promote its transformation into gaseous hydrochloric acid. The filters with Cl^-/Na^+ ratios above 1.81 coincided with the six winter days when it became clear that the Cl^- detected in the schoolyard came from sources other than sea salt. Despite the predominant air mass trajectories being over the ocean (**Fig. S5**), the winds on these six days came mainly from the continental area. These findings support the conclusion that Cl^- at the school was primarily of marine origin during most of the sampling period but also suggest that other processes influenced chloride levels on specific days.

Mineral dust accounted for a higher proportion of PM_{10} mass in the classroom than in the schoolyard in winter. However, this percentage was lower in winter than in spring (Table 3). The predominant elements were Ca, Al and Fe (Table 4). The average concentration of Ca and Al was higher indoors (0.60 and 0.26 μg m^{-3}, respectively), while the concentration of Fe was higher outdoors (0.21 μg m^{-3}). MD levels in classrooms accounted, on average, for PM_{10} mass fraction of 20% in winter and 35% in spring, values that were lower than those in other studies. For example, Sánchez-Soberón et al. [80] reported that mineral matter contributed 55% of PM_{10} in the cold season and 44% in the warm season in a study conducted in 12 schools in Catalonia. On the other hand, in a study in two schools located in urban areas of Malaysia for over 9 months in 2012, Mohamad et al. [38] found that the mineral fraction contributed between 27% and 31% of PM_{10}. These differences can be attributed to several factors, sampling duration in each study, the specific meteorological conditions, and the characteristics of the study sites. For example, schools in Spain and Malaysia were notably affected by traffic emissions, and the use of chalk in classrooms was a common practice at that time, both of which likely influenced the results, as it has been shown that in classrooms that use chalk, average concentration double [14]. Furthermore, it was verified that the Ca/Al ratio in the classrooms and in the schoolyard was higher in winter (4.1 and 3.8, respectively) than in spring (2.4 and 1.2, respectively), suggesting the presence of an additional source of Ca, mainly in the classrooms. This could be linked to an increase in the resuspension of dust transported on the soles of children's shoes from the schoolyard, especially since the classroom windows were kept closed for most of the season.

Table 4
Summary of PM_{10} concentrations and its chemical constituents.

	Indoor				Outdoor			
Species	n	Mean	Min	Max	n	Mean	Min	Max
μg m^{-3}								
PM_{10}	35	25.2	11.3	45.5	31	27.3	9.85	51.7
OC**	35	5.53	2.30	16.8	30	3.64	0.24	18.1
EC	34	0.88	0.04	3.80	31	0.97	0.01	5.64
Al	33	0.26	0.05	1.35	31	0.23	4×10^{-3}	0.95
NH_4^+	35	0.25	0.02	0.89	31	0.23	4×10^{-3}	0.75
Ca**	35	0.60	0.07	1.60	31	0.26	0.09	0.82
Cl^-	35	1.29	0.11	4.98	31	1.62	0.13	5.50
Fe**	35	0.14	0.05	0.54	34	0.22	0.06	0.57
F^-	30	0.07	0.05	0.12	27	0.07	0.05	0.12
K	33	0.15	0.02	0.59	31	0.20	0.01	0.75
Mg**	35	0.13	0.03	0.38	31	0.19	0.02	0.43
Na**	35	0.91	0.09	3.00	31	1.42	0.17	3.44
NO_3^-**	35	0.77	0.13	1.84	31	1.42	0.13	3.35
S**	35	0.30	0.10	0.57	31	0.43	0.16	0.68
SO_4^{2-}**	35	0.76	0.17	1.65	30	1.16	0.41	2.16
ng m^{-3}								
Ti**	34	22.1	3.75	75.7	28	15.4	3.81	47.3
As	35	0.82	0.12	2.93	31	0.75	0.17	2.12
Ba	34	13.6	1.47	132	31	14.5	1.52	75.3
Cr**	35	1.51	0.56	3.23	29	1.97	0.48	3.62
Cu	35	5.61	1.27	36.6	31	7.73	1.33	37.0
Mn	30	4.21	3.75	8.41	30	5.42	3.78	11.8
Pb	35	4.89	0.52	20.1	31	6.59	0.54	20.3
Rb	35	1.10	0.20	3.63	31	1.42	0.25	4.54
Sb	35	1.30	0.22	4.66	31	3.05	0.25	16.9
Sn	35	1.52	0.20	6.18	31	1.93	0.07	6.10
Sr	35	1.83	0.55	3.67	31	2.07	0.11	6.10
∑ other trace elements[i]		2.39	0.41	8.64		3.27	0.32	11.1
Arabinose	29	41.7	10.6	254	28	17.4	10.0	94.3
Glucose	27	9.83	1.59	22.2	26	13.7	1.30	35.8

n: Number of samples.
** Indicates a statistically significant difference between indoors and outdoors (p-values < 0.05).
[i] Elements detected in at least 28% of the filters at each site were considered. Indoor: Bi, Cd, Ce, Cs, La, Li, Nb, Nd, V, W; Outdoor: Bi, Cd, Ce, Cs, La, Li, Nb, Nd, Se, Th, V, W.

Trace elements accounted for less than 1.5% of the PM_{10} mass, with Ba, Ti, Pb, and Cu being among the top 4 contributing elements in both environments and seasons. The average levels of Ba, Cu, and Pb were highest in the outdoor environment (Table 4), with Ba and Pb concentrations peaking in winter, while Cu levels were highest in spring. Other trace elements such As, Ba, Cu, Rb, Sb, Sn, Sr, and V were found in all classroom and schoolyard samples in both seasons. Mn was detected in all indoor and outdoor samples in winter, while Cs, Ga, La, Nb, Nd, and Se were detected in all spring samples.

The component "Other" refers to unidentified aerosol constituents, which, in part, can result from errors in gravimetric and chemical quantifications. However, it is likely that much of the unaccounted mass consists of absorbed water. This is particularly relevant since the total mass of PM_{10} was measured under controlled conditions (20 °C and 50 % RH), which could influence the interaction between the laboratory's atmospheric water vapour and the particulate matter on the filters, as reported in other studies [39]. In general, the unaccounted mass was high outdoors in winter and low indoors.

3.2. PM_{10} chemical composition

3.2.1. Ions

Concentrations of water-soluble anions (Cl^-, NO_3^-, SO_4^{2-}, F^-) and cations (NH_4^+, Na^+, K^+, Ca^{2+}, Mg^{2+}) are displayed in Fig. 3. Both indoors and outdoors, the dominant ionic species were Cl^-, NO_3^- and SO_4^{2-}. The highest concentrations were observed in the schoolyard in spring (mean: 4.84 μg m^{-3} for anions and 2.59 μg m^{-3} for cations). Due to the intensification of photochemical activity, nitrate and sulphate concentrations were higher in this season than in winter, both indoors and outdoors. In the schoolyard, the average concentrations of these two ions were 2.2 and 1.6 times higher in spring compared to winter, while the mean concentrations of NH_4^+ and K^+ were found to be higher in winter. The highest levels of NO_3^- and SO_4^{2-} were observed on the same day in spring, when air masses that had originated from the Cantabrian Sea 48 h earlier crossed northern Spain and Portugal before reaching the school. In contrast, during winter, the peak concentration of NH_4^+occurred when the air masses had passed over the Atlantic Ocean and parts of northern Portugal.

The equivalent cation/anion (C/A) ratios ranged between 0.8 and 2.7 in the classrooms and between 0.9 and 1.8 in the schoolyard (**Fig. S6**). The highest C/A ratio (2.75) was observed during winter and coincided with the day when the highest Ca^{2+} (0.28 μg m^{-3}) and the lowest Cl^- concentrations were recorded at the school. Ca^{2+} often comes from calcium-containing compounds like calcium carbonate ($CaCO_3$), which can be a significant source of calcium in the atmosphere, especially in dust or soil particles. The presence of CO_3^{2-} creates a C/A ratio, with a dominance of Ca^{2+} over anions, like Cl^-. Conversely, the lowest C/A ratio of 0.8 was recorded on a different winter day, when SO_4^{2-} and Cl^- concentrations were higher in the classroom's indoor air. This low C/A ratio, coupled with an I/O ratio of less than 0.4, suggesting that external sources, rather than indoor activities, were the primary contributors to

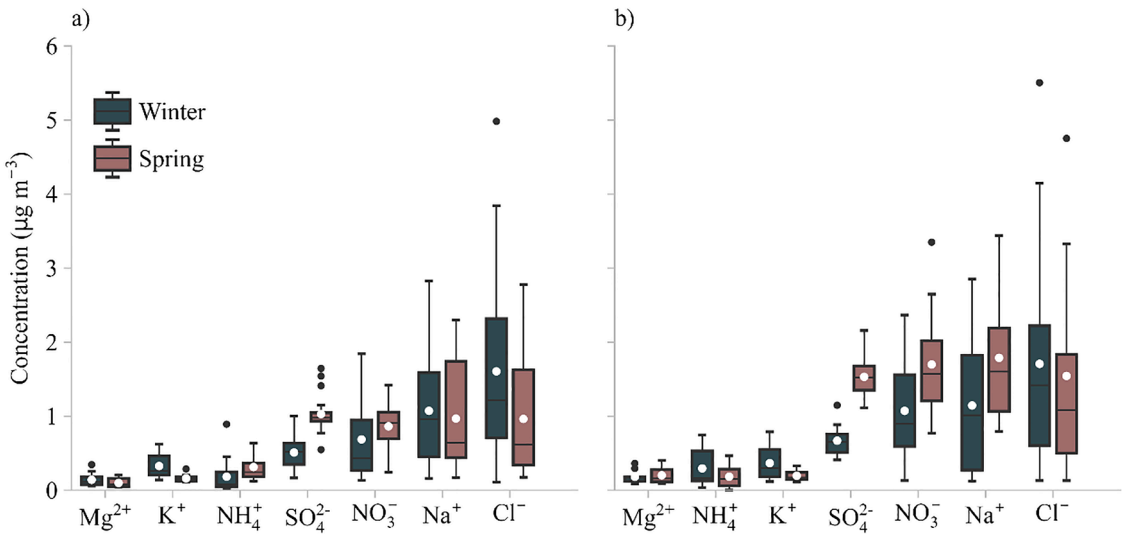

Fig. 3. Concentrations of water-soluble ions in PM_{10} collected in (a) classrooms and (b) schoolyard.

the PM_{10} levels on that day.

Overall, the NO_3^-/SO_4^{2-} ratio at the school averaged 1.12 (**Fig. S6**), suggesting that nitrate is slightly more prevalent than sulphate in the area, likely due to a combination of local traffic, industrial emissions, and photochemical processes. However, it is noteworthy that on certain winter days, higher ratios (>1.5) were recorded, while on other occasions during both winter and spring, the ratios were lower (<0.5), reflecting the complex interplay between local emissions, meteorological conditions, and long-range transport of pollutants. On days with more traffic and combustion, the ratio is higher, while on days with increased industrial emissions, sulphate transport, or wet conditions, the ratio tends to be lower. These fluctuations highlight how dynamic and context-dependent air quality can be.

3.2.2. *Carbonaceous fraction*

Total concentrations of EC and OC at the school peaked during the winter. Indoor OC levels consistently exceeded outdoor concentrations across both seasons (Fig. 4). When outdoor OC was modelled as the

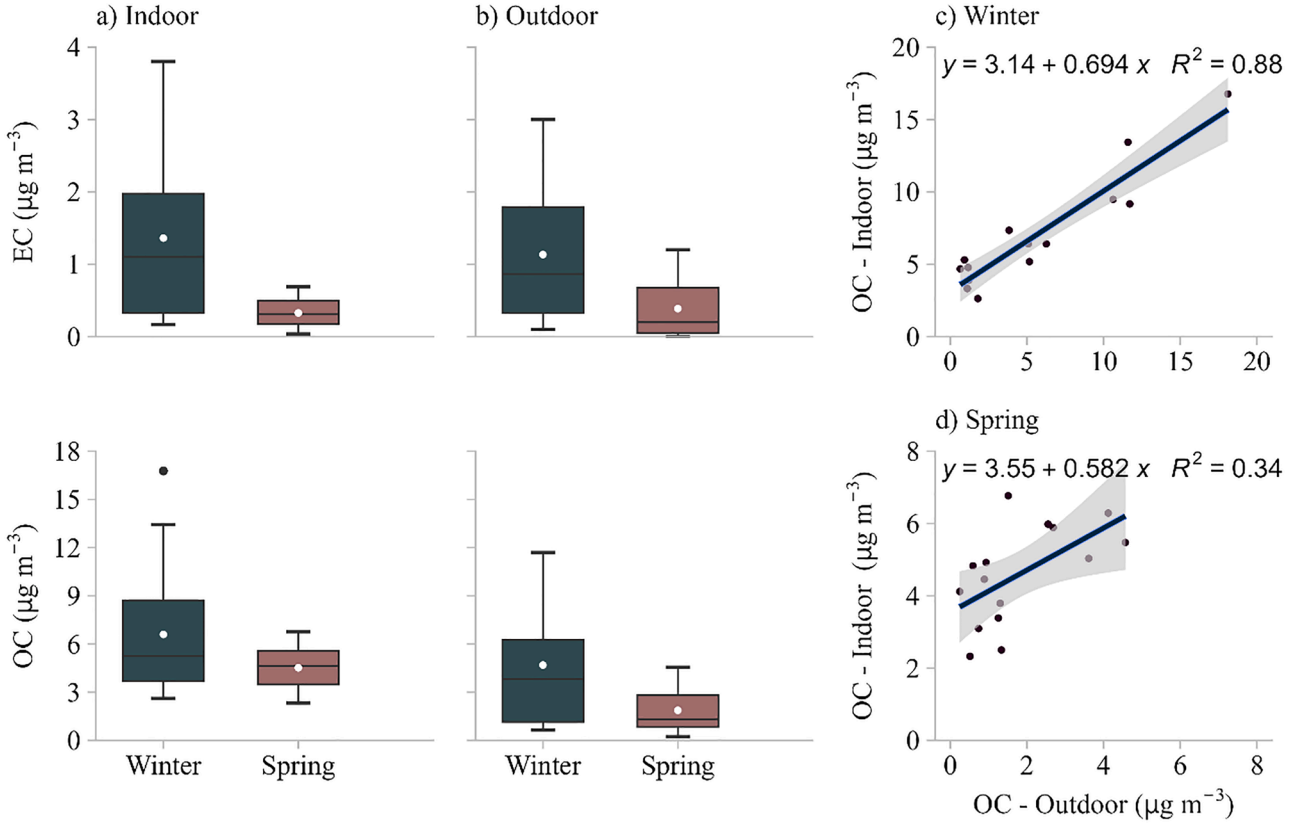

Fig. 4. Concentrations of carbonaceous fractions of PM_{10} (a and b), and scatter plot of the concentrations of OC in classrooms versus those in the schoolyard in winter (c) and spring (d), the line was obtained by linear regression. Different scales have been included to facilitate visualisation. The whiskers are the 5th and 95th percentiles, the black dot indicate the maximum value, the lines in the middle of the boxes represent median values while mean values are shown as white dots.

dependent variable to predict indoor levels (Fig. 4c-d), the y-intercepts of the linear correlations indicated that a significant portion of OC was generated from internal sources. While indoor and outdoor OC showed a very high degree of correlation in winter (R^2 = 0.88, n = 14), this relationship weakened in spring (R^2 = 0.34, n = 16). The high degree of correlation in winter indicated that OC in classrooms and the schoolyard originated from common sources; however, the slope (up to 0.694) indicates that outdoor concentrations increased less rapidly than indoor levels, further pointing to indoor accumulation. The same pattern has also been reported in other studies [40,41] and has been associated with internal sources. In addition, poor ventilation can lead to the accumulation of OC; indeed, as verified in our previous work [16], these classrooms had inadequate air exchange in both winter (0.32 to 1.44 h^{-1}) and spring (0.34 to 1.56 h^{-1}). This is a critical observation, as Li et al. [42] suggested that even enhancing ventilation, by opening windows for durations ranging from hours to an entire day, cannot effectively decrease the concentration of semi-volatile organic compounds (SVOCs) in indoor air, despite their primary emission sources being indoors.

Consequently, the correlation between indoor and outdoor OC during winter likely stemmed from residential heating activities, which contributed significantly to OC levels in the schoolyard. Conversely, the spring data suggest that the OC remaining in the classrooms was primarily related to internal sources. Although the thermo-optical method primarily quantifies OC in the particulate fraction, indoor OC cannot be solely attributed to combustion-related sources. In classroom environments, several non-combustion processes contribute to OC levels, including the infiltration of outdoor particles, resuspension of organic-rich settled dust (e.g., skin flakes, textile fibres, and soil particles transported indoors), and the formation of secondary organic aerosol from reactions involving volatile organic compounds emitted by cleaning products, building materials, and occupant-related activities [43,44]. Thus, even in the absence of indoor combustion, it is possible to account for OC originating from active internal sources.

In contrast, indoor EC concentrations appeared to be primarily driven by outdoor infiltration. This is supported by the I/O ratios, where only 30% of EC samples were showed ratios higher than 1.5 in both seasons, while the I/O ratio of OC ranged from 0.80 to 7.22 in winter and from 1.20 to 16.9 in spring (**Fig. S7**).

EC and OC revealed a different seasonal correlation pattern (**Fig. S8**). Outdoors, OC and EC show a very high degree of correlation in winter (R^2 = 0.95), suggesting that the carbonaceous fractions in the schoolyard share common sources or were influenced by similar processes during the coldest days. However, this correlation significantly weakened in spring (R^2 = 0.60), highlighting lower influence of primary combustion sources on the formation of both carbonaceous particle categories in this season. The same pattern was observed indoors, although with lower correlations (R^2 = 0.76 in winter and R^2 = 0.45 in spring). Throughout the field samplings, OC/EC ratios in the schoolyard ranged from 1.81 to 33.8, while the variation in classrooms was from 2.49 to 98.9 (**Fig. S7.a**). Overall, linear regression analysis between PM_{10} and OC indicate that this carbonaceous component can better explain the variation in PM_{10} indoors than outdoors (R^2 = 0.60 and 0.40 in winter and spring, respectively) (**Fig. S9**). EC explains more of the variance in PM_{10} levels in winter (R^2 = 0.51 in classrooms and R^2 = 0.70 in the schoolyard). In contrast, no correlation was observed between these variables at either site in spring (**Fig. S9**).

The levels of OC and EC in both school environments were like those reported in the literature for other educational settings Leppänen et al. [45]. However, the OC/EC ratios in this study exhibited greater variation compared to those observed in other schools. OC/EC ratios ranging from 18 to 28 in Lisbon [35] and from 10 to 19 in South Korea [46] were observed in PM_{10} samples collected from classrooms [47]. observed that OC/EC ratios were higher in residential homes than outdoors. The authors attributed the elevated OC/EC ratios to the significant formation of secondary organic aerosols which increases the amount of OC in the indoor environment. Studies suggest that the OC/EC ratio can vary considerably depending on the measurement location (rural, urban, industrial), as well as the sources (primary and secondary) [48].

3.2.3. Metal(loid)s

A total of 58 metal(loid)s were quantified in the samples. Si concentration was estimated by multiplying the Al concentration by 3.92, based on the typical Si/Al ratio observed in crustal materials, where Si and Al are major components. The concentration of these elements in the schoolyard ranged from 1253 to 9046 ng m^{-3}, while in the classrooms it varied from 681 to 10,084 ng m^{-3} (Fig. 5). During winter, the mean total element concentrations at both school environments were very close (2948 ng m^{-3} indoors and 2746 ng m^{-3} outdoors). In contrast, in spring, total element concentration increased, with levels in classrooms rising 1.43 times higher and in the schoolyard 1.82 times higher than those measured in winter. Concentrations of PM_{10}-bound As, Sn, Bi, Ti, Al and Ca were higher indoors in both seasons (Fig. 5), while S, Fe, Mn, V, Cr and Ba showed similar average values in the two environments (I/O ~1). In both seasons, the enrichment of elements such As, Ni, Cr, W, As, S, Cu, Pb, Sn, Se, Cd, Bi and Sb (EF > 10) at the two environments suggested an anthropogenic origin. In contrast, elements like Al, Ca, La, Li, Mn, Nb, Nd, Ti, and V exhibited low enrichment (EF < 10), indicating a crustal origin in both the classrooms and the schoolyard (**Fig. S4**). When Alves et al. [49] investigated the composition of $PM_{2.5}$ in the same city, they observed not only the enrichment of Pb, Cd, Cu, Sn, Se, Bi and Sb, but also Zn, B and Mo. The researchers attributed this enrichment to the contribution of industrial emissions and major roads near the sampling site. However, in this study, B was not detected, and Zn and Mo were only found in a few samples. Although residential biomass combustion is a common practice in the region, the EFs for K did not reveal the dominance of this source. However, it should be noted that the lack of K enrichment in PM_{10} filters could be affected by a combination of factors, such as the type of biomass burned, the combustion temperature and the efficiency of the process [50].

Significant correlations among the chemical species were observed. In classrooms, As showed positive significant correlations with Bi, EC, OC, Cu, K, Pb, Rb and Sb, indicating a possible shared anthropogenic source, such as the burning of fossil fuels or the use of lead-based building materials. Fe was correlated with Al, Ca, Cu, Li, Rb, Ti and V, indicating dust resuspension. These patterns reinforce the hypothesis that PM_{10} in classrooms result from a combination of natural and anthropogenic sources. Al, As, Ba, Bi, Ca, Ce, Fe, Li, S and Nb were linked with several species. Additionally, As correlated with Cd (ρ = 0.72), a pattern also observed in classrooms, and associated with mixed sources such as diesel combustion and industrial emissions [51].

The number of elements detected in the spring filters was higher compared to those from the winter sampling. The variability between the two seasons suggests that both human activities and meteorological conditions, such as the decrease in accumulated precipitation during the sampling campaigns (193 mm in winter and 17 mm in spring during sampling campaigns) and the increase in mean wind speed (1.05 m s^{-1} in winter, 1.48 m s^{-1} in spring), played a significant role in the concentration and correlation of metals in the indoor and outdoor environments of the school. Notably, no Saharan dust intrusion was detected on any day neither in winter nor in spring (**Fig. S5**). However, in spring, ~73% of the air masses passed through the industrial estate (5 of the 8 clusters, **Fig. S5**). This could have resulted in a higher metal(loid) load in PM_{10} during this season. Likewise, these outdoor pollution sources contribute to indoor element concentrations, especially when classroom windows are opened more frequently in spring than in winter.

Despite the detection of potentially health-hazardous heavy metal (loid)s such as Cr, Mn, Cu, Zn, As, Pb, Cd and Co. In particular, the levels of Ni, As, Cd and Pb were below the recommended annual average values set out in Directive 2024/2881 [52], under the revised directive [53], the annual average concentrations are now established as 20 ng m^{-3}, 6 ng m^{-3}, 5 ng m^{-3} and 0.5 μg m^{-3}, respectively.

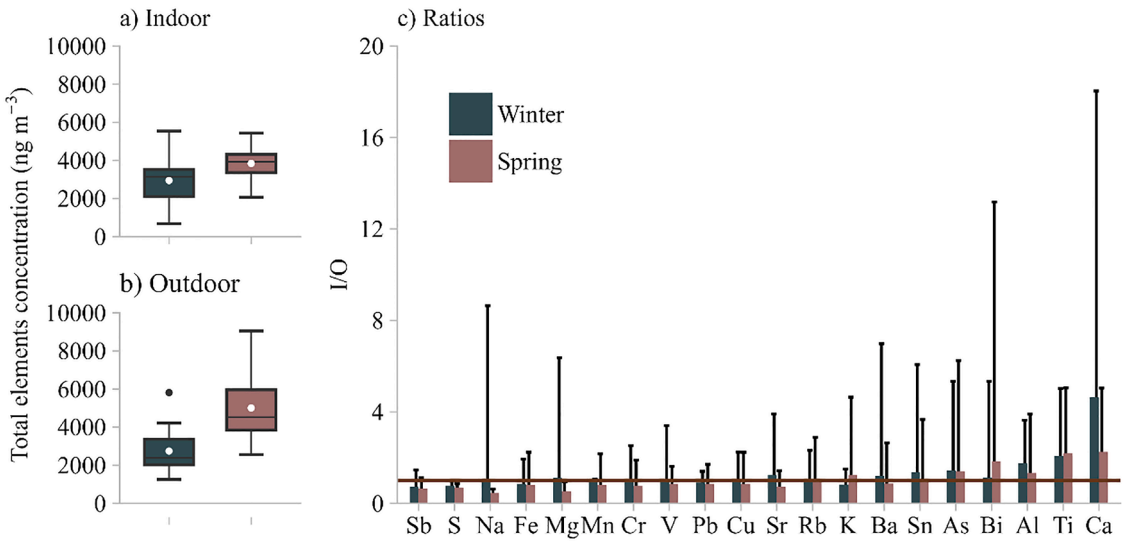

Fig. 5. Statistics of the daily average concentrations of the total chemical species in both seasons: (a) classrooms; (b) schoolyard. The whiskers represent P5 and P95, and the line in the middle correspond to the median, while the white dots represent the mean. The data considers the 58 chemical species detected in the PM_{10} samples, including 10 from outside and 13 from inside that were present in only 23% of the filters from both school environments. (c) Average I/O ratios categorised by season. The values are sorted by average. Error bars represent the maximum value.

3.2.4. *Sugar compounds*

The following saccharides and anhydrosaccharides were quantified in the school samples: mannose, fructose, sucrose, glucose, arabinose, galactosan and levoglucosan. Arabinose and glucose were detected in at least 71% of the samples, both indoors and outdoors. Arabinose was by far more abundant in classrooms (65.0 ± 85 ng m^{-3}), while glucose was higher in the schoolyard (23.5 ± 8.75 ng m^{-3}). Levoglucosan and galactosan were detected in 6 and 16 samples from the schoolyard, with average concentrations of 203.8 ± 112 and 16.9 ± 21.8 ng m^{-3} respectively, while in the classrooms they were detected in only 5 and 11 samples, respectively.

The mean daily concentrations of all sugars in PM_{10} ranged from < LOD to 509 ng m^{-3} in the schoolyard and from < LOD to 653 ng m^{-3} in the classrooms. No statistically significant differences in concentrations of these sugars were found between the classrooms and the schoolyard. However, a much higher daily mean concentration of total sugars was recorded in winter (135 ± 167 ng m^{-3}) compared to spring (38.4 ± 33.6 ng m^{-3}). At the schoolyard, anhydrosugars exhibited the highest average concentrations (48.2 ng m^{-3}), while in the classroom, saccharides were more prevalent, reaching an average of 63.3 ng m^{-3}. In addition, significant differences in galactosan, glucose and mannose levels were observed between both seasons (**Table S3**).

Sugar levels have been reported for a few European school environments [34,54]. In general, the concentrations of sugar compounds reported in these studies are higher than those obtained in the present investigation. Alves et al. [34] observed higher concentrations of levoglucosan inside a primary school classroom in central Aveiro, Portugal (February - May 2011), while in this study that anhydrosugar was not detected in any classroom samples in spring. Fructose levels in Aveiro were up to 8 and 3 times higher than those quantified indoors and in the schoolyard in Estarreja, respectively. According to Oduber et al. [55], anhydrosugar concentrations during cold seasons may result from increased use of domestic heating appliances. In contrast, some saccharides, which are more commonly emitted as primary biogenic aerosol particles (e.g., bacteria, plant fragments, chemical species, pollen, and fungal spores), are typically more abundant in warmer seasons. However, fructose, glucose and arabinose have also been observed in smoke samples from biomass burning [55]. In this study, during winter, levoglucosan, galactosan and arabinose were significantly correlated with biomass burning, traffic and fuel combustion markers, such as K, OC, EC and Rb. Glucose was correlated with several elements but not with any sugar. Sucrose and fructose were only correlated with each other, suggesting a common origin. In spring, sucrose and fructose were correlated with Ca, Ti and glucose, indicating that dust intrusions may have been the emission sources in that period. However, glucose was also correlated with many other elements, such as Cs, Fe, K, V, etc., suggesting that there may be additional sources beyond dust. In summary, fructose and sucrose at the school may be related to plant activity, while arabinose, glucose and levoglucosan could be associated with a mix of sources such as biomass burning and traffic.

3.3. *Source contribution to PM_{10}*

3.3.1. *Pollution sources in classrooms*

Six components explained 88% of the variance in the PM_{10} dataset (**Table S4**). The first component (Fig. 6), which accounted for 21.6% of the total variance, had strong loadings of Al, Fe, Ti and *Sc*. Al, Fe and Ti are among the most abundant elements in the Earth's crust [56,57]. When these elements appear together as a component, they typically indicate a crustal or mineral dust source. This suggests a combination of outdoor soil intrusion and indoor resuspension of geologically derived material from local sources, especially since no long-range transport from the Sahara Desert was detected during the sampling period. In classroom environments, this component is likely influenced by student movement and cleaning activities, which can resuspend particles that originally entered from outdoors [58]. Natural ventilation also facilitates the infiltration of wind-blown soil dust [59].

The second component indicates a biomass burning source, as evidenced by high loadings of OC, EC, and K, all of them well-established markers for this source [60,61]. In addition, loadings of Pb, As and Sb were also observed. These elements further support the origin of this source, since As and Pb can be present in biomass before combustion [62], and combustion residues like wood ash are often enriched with these toxic elements. In a study on ashes produced from burning wood biomass in closed wood-fired furnaces, Smołka and Jabłońska [62] concluded that levels of As and Pb were significantly higher than those of other metals such as Cd, Cu, Zn, and Cr. In the present study, the high EFs observed for these elements indicate an anthropogenic source, especially in winter (**Fig. S4**), consistent with increased residential wood burning during colder months. However, it is important to note that Pb is also associated with other combustion sources, such as waste incineration [64]. Also, metal(loid)s such As and Sb remain retained

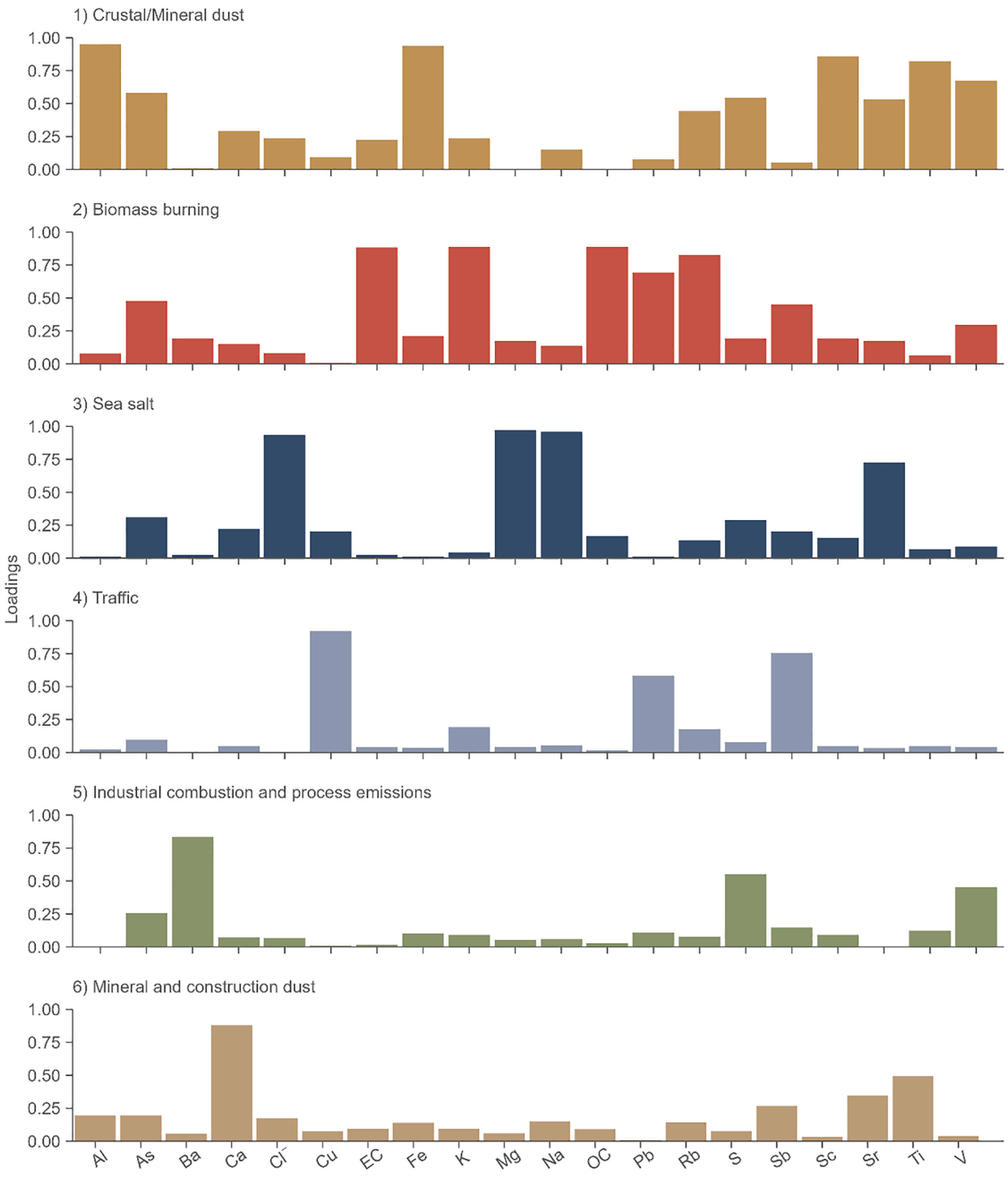

Fig. 6. Loadings of chemical species for each factor identified in classrooms.

primarily in the bottom ash generated by waste incineration [63].

The third component corresponded to a marine profile, mainly explained by Na, Cl and Mg. While cleaning products used in classrooms may contain sodium and chlorine, their influence appears negligible, as the overall elemental profile remains consistent with that of natural sea salt, as previously discussed. The school's coastal location supports the marine air mass intrusion from the Atlantic Ocean, a pattern further corroborated by the air mass trajectory analysis (**Fig. S5**). The detection of this marine component in classroom air suggests outdoor-indoor air exchange. As noted earlier, the Cl^-/Na^+ mass ratio was approximately 1.8, consistent with unmodified sea salt.

The fourth component explained 9.30% of the total variance and is primarily characterised by high loadings of Cu, Sb and Pb. This component was attributed to vehicular traffic, as brake pad wear has been identified as a key source of Sb emissions [63], while Cu and Pb are commonly used in tyre [65]. These findings support the association of Cu, Sb, and Pb are with vehicular traffic in PM samples, primarily due to brake and tyre wear.

In the fifth component, Ba, V and S were the only elements with prominent loadings, suggesting a complex source profile likely dominated by industrial and combustion-related emissions. V is a well-well-known marker of heavy fuel oil combustion, typically associated with emissions from power plants or industrial boilers burning residual oils [66]. In Estarreja, local industry is the more probable source, especially given the proximity of industry facilities near the school. S is strongly associated with the combustion of fuels such as coal and heavy oil [67]. Although S can also be present in secondary aerosols, its loading here alongside V and Ba suggests a primary or combustion-related origin. Industrial emissions from the Estarreja estate are a likely contributor. Ba is commonly linked to non-exhaust traffic emissions, especially brake wear [68], but it can also be emitted from some industrial processes [69]. This component was labelled as “industrial combustion and

process emissions", likely reflecting the influence of nearby petrochemical activities in Estarreja.

The last component was dominated by Ca, with minor contributions of Ti, Sr, and Sb. Ca is a marker of construction dust and building materials, particularly cement and concrete [70]. In indoor settings such as classrooms, elevated Ca levels are often linked to the degradation and erosion of structural elements, including walls, floors, ceilings, and windowsills, as well as the infiltration of outdoor road dust [58]. Ti, commonly found as titanium dioxide (TiO_2), is widely used as a pigment in white paints and plasters. Although Ti is also a minor crustal element, its presence here likely reflects contributions from interior surface materials or the resuspension of settled indoor dust, as reported in a previous study conducted in different environments [71]. Sr can be naturally co-released with Ca from minerals such as gypsum and limestone [72] and is frequently found in PM from school settings [59,70]. Sb, while typically associated with brake wear and vehicular emissions [68], may indicate indoor contamination from traffic sources through non-exhaust emissions that have penetrated the classrooms.

The contributions estimated by the APCS-MLR model are presented in **Fig. S10**. A moderate correlation was observed between the modelled and measured PM_{10} concentrations. The first four components accounted for most contributions to PM_{10}. On average, the first component accounted for 27.8% of the total PM_{10}, while the sixth component contributed 10.3%. In contrast, the component related to industrial combustion and process emissions had the lowest contribution (<1%).

3.3.2. *Pollution sources in the schoolyard*

In the schoolyard, six major sources of PM_{10} were identified (Fig. 7), with the first four resembling those found in classrooms, albeit with different contribution percentages. The remaining two components were attributed to SIA and emissions from industrial activities. Together, these six components explained 91.5% of the total variance in the analysed data (**Table S4**).

SIA formation was observed exclusively outdoors, likely because

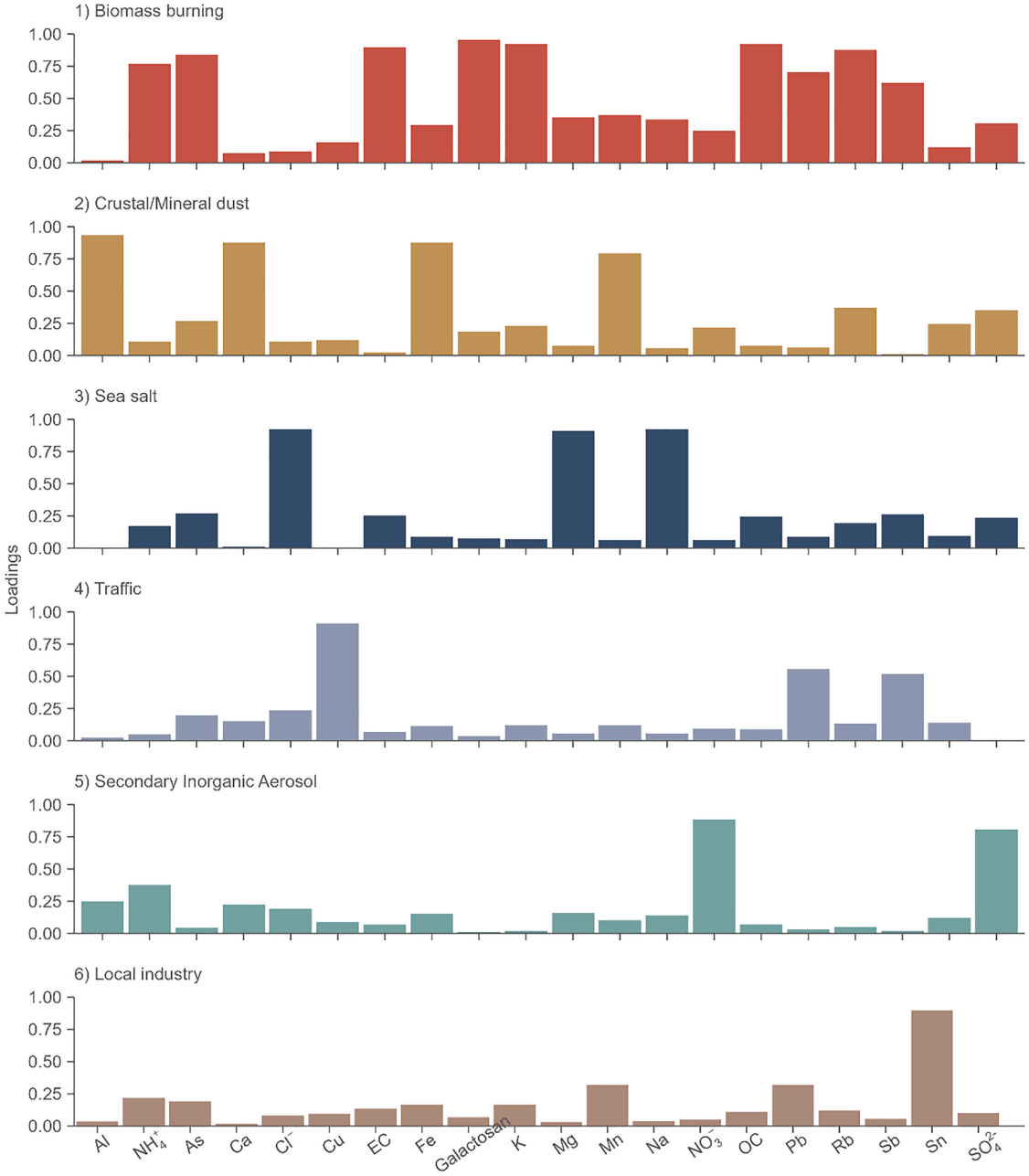

Fig. 7. Loadings of chemical species for each factor identified in the schoolyard.

atmospheric conditions (like high humidity) and the presence of precursor gases are essential for the secondary chemical reactions [73]. Average I/O of 0.72 for SO_4^{2-} and 0.83 for NO_3^- were observed during winter, decreasing to 0.65 and 0.49, respectively, in spring, indicating higher concentrations of these ions in outdoor air. The decrease in their I/O ratios from winter to spring suggests increased outdoor photochemical activity and dispersion in spring. In contrast NH_4^+ showed a lower I/O ratio in winter (0.83), which increased substantially in spring (I/O = 4.99), suggesting a greater relative indoor presence during the warmer season. Warmer conditions enhance microbial activity on the skin and in sweat, leading to greater breakdown of nitrogen-containing compounds into ammonia. Studies suggest [74–76] that SIA form primarily in the outdoor atmosphere and that, although they can infiltrate indoors, concentrations are typically lower in the latter due to factors such as the lack of favourable conditions for their formation.

The final component was characterised by high loadings of Sn, Pb, and Mn. This component indicates a local industrial source, likely associated with metal processing or other industry emissions. Sn has been identified as a common element in metalworking and soldering environments [77]. It is often emitted during the manufacture or use of organotin compounds, metal plating, or production of alloys. Pb emissions in industrial regions are often tied to metal smelting, battery recycling, or chemical manufacturing [78]. Mn is commonly associated with steel manufacturing and industrial combustion [30]. The presence of Mn in this context is indicative of industrial metallurgical and chemical emissions. These emissions are specific to outdoor air, with no significant presence detected indoors. According to the wind rose (**Fig. S1**), prevailing winds during the spring season coming from the nearby industrial estate could potentially transport some of the elements identified in this component toward the schoolyard.

On average, the combustion-related source contributed approximately 27.8%, followed by sea salt (component 3) with 20.4%, SIA with 12%, and mineral dust with 7.02% (**Fig. S10**). Additional sources, corresponding to industrial activity and traffic, contributed less than 2%. The regression model presented a coefficient of determination (R^2) of 0.86, indicating good agreement between the calculated and observed values. Furthermore, four of the six sources (components 1, 2, 3, and 5) showed statistically significant regression coefficients ($p < 0.05$), reinforcing the relevance of these sources in explaining the variability of PM_{10} observed in the schoolyard.

4. Study strengths and limitations

This study provides valuable insights into the characterisation of PM_{10} under real school conditions in two seasons. However, these campaigns may correspond to relatively elevated pollution conditions, and thus the results may not fully represent the full annual variability. Future research should encompass a complete annual cycle to accurately identify high- and low-pollution seasons and to evaluate seasonal variations in PM_{10} sources. In addition to the sampling limitations, the lack of suitable source markers decreases the ability of the PCA to correctly identify the sources impacting the receptor site. This is because the number of variables considered in the factor analysis is conditioned by the number of observations available. The elements emitted by two or more principal components influence the principal component scores, which, in turn, affect the contributions of those source categories to the total PM_{10} modelled. Due to this limitation, 32% in the schoolyard and 26% in the classrooms could not be attributed to any possible source by this technique. In addition, the profiles of most PM_{10} sources are not completely stable over time, which can complicate the interpretation of the derived sources.

Despite using backward trajectories, it could not be determined whether the industrial estate significantly impacts the PM_{10} levels reaching the schoolyard, since the fact that winds during both sampling periods passed through the industrial area at some point does not necessarily imply that pollutants reached the PM_{10} sampler. Topography and buildings around the school could influence the direction and intensity of air masses, thus affecting their arrival at the schoolyard.

5. Conclusions

On average, PM_{10} concentration in classrooms remained below the new World Health Organisation (WHO) recommended value of 45 μg m^{-3}. However, even when daily values were below this guideline, 94% of these samples exceeded 15 μg m^{-3}, suggesting that the annual average may still surpass the WHO recommended threshold and the limit set by the new European Directive. In contrast, concentrations of hazardous pollutants such as Ni, As, Cd, and Pb remained below the thresholds established by Directive 2024/2881, both indoors and outdoors, in both seasons.

This study fills a geographic gap by characterising a school environment near an industrial estate, revealing that its primary pollution sources are consistent with broader national trends. The identification of biomass burning, dust, and sea salt as dominant sources, suggests that factors such as meteorology, the specific duration of the field campaign, and common urban activities can exert influence on air quality at the school overshadowing local industrial contributions. Indoor dust was specific to classrooms, while secondary aerosols were more common outdoors. Biomass burning was the largest contributor, accounting for over 17.6% in both settings. Industrial activity appeared to have a little impact, possibly due to prevailing wind patterns and the short duration of the sampling campaigns. Longer-term studies across all seasons are needed to better understand these effects. Such studies are also essential to assess whether daily concentrations of PM_{10} and the previously mentioned hazardous pollutants consistently comply with recommended limits throughout the entire school year, and to determine whether there is seasonal variability in the contribution of the identified sources.

The results shed light on relevant aspects affecting air quality in the school environment. While EC, Cl^-, Na, NO_3^- and SO_4^{2-} mainly impact outdoor air, species such as OC, Ca, Al, and Ti have a greater influence indoors. Although interventions may be challenging, air quality in schools could be improved by adapting and applying some strategies already proposed and tested in scientific research, such as implementing a targeted ventilation and air purification protocol on alert days, installing balanced mechanical ventilation with heat recovery and particle filtration to ensure optimal indoor air quality and enforcing green barriers as a complementary measure to improve school air quality. Cooperation between research institutes, policymakers, and school staff is also essential to support the development of these strategies. Such efforts can also help align key United Nations Sustainable Development Goals (SDG 3, SDG 4, SDG and SDG 11).

Funding

This work was partially financed funded by national funds through FCT – Fundação para a Ciência e a Tecnologia I.P., under the project/grant UID/50006 + LA/P/0094/2020. In addition, partial financial support was received from the LabEx-DRIIHM-OHM programme (CNRS – INEE, France), within the STOP project - Source drivers of (eco) TOxicity of airborne Particles in school environments in Estarreja: Strategies for minimising the risks.

CRediT authorship contribution statement

Isabella Charres: Writing – review & editing, Writing – original draft, Visualization, Methodology, Formal analysis, Data curation, Conceptualization. **Yago Cipoli:** Writing – review & editing, Methodology. **Estela D. Vicente:** Writing – review & editing, Methodology. **Leonardo Furst:** Methodology. **Teresa Nunes:** Writing – review & editing, Methodology. **Ana M. Sánchez de la Campa:** Methodology. **Manuel Feliciano:** Writing – review & editing, Supervision,

Conceptualization. **Célia Alves:** Writing – review & editing, Supervision, Funding acquisition, Conceptualization.

Declaration of competing interest

The authors declare the following financial interests/personal relationships which may be considered as potential competing interests: Celia Alves reports financial support was provided by Centre National de la Recherche Scientifique (CNRS), Epigenetic and Parasites Team - LABEX ParaFrap. Reports a relationship with that includes:. Has patent pending to. If there are other authors, they declare that they have no known competing financial interests or personal relationships that could have appeared to influence the work reported in this paper.

Acknowledgements

The authors would especially like to thank the school principal and teachers, who have willingly participated in this study. This work was partially financed funded by national funds through FCT – Fundação para a Ciência e a Tecnologia I.P., under the project/grant UID/50006 + LA/P/0094/2020. FCT is also acknowledged for providing grants to the PhD fellows I. Charres (DOI:10.54499/2022.12142.BD), Y. Cipoli (SFRH/BD/04992/2021) and L. Furst (SRFH/BD/08461/2020), as well as for the research contract under Scientific Employment Stimulus to Estela D. Vicente (DOI:10.54499/2022.00399.CEECIND/CP1720/CT0012). The authors thank Diana Costa from the University of Aveiro for her support in some analytical tasks. This work was performed within the STOP project - Source drivers of (eco) TOxicity of airborne Particles in school environments in Estarreja: Strategies for minimising the risks, – funded by the LabEx-DRIIHM-OHM programme (CNRS – INEE, France).

Supplementary materials

Supplementary material associated with this article can be found, in the online version, at doi:10.1016/j.buildenv.2026.114692.

Data availability

Data will be made available on request.

References

[1] P. Sicard, E. Agathokleous, A. De Marco, E. Paoletti, V. Calatayud, Urban population exposure to air pollution in Europe over the last decades, Environ. Sci. Eur. 33 (2021) 28, https://doi.org/10.1186/s12302-020-00450-2.

[2] A.K. Collison, M.A. Byrne, J.A. McGrath, Indoor air quality in naturally ventilated classrooms and offices in Ireland, Build. Environ. 279 (2025) 113023, https://doi.org/10.1016/j.buildenv.2025.113023.

[3] B. Du, J.F. Rey, M. Cesari, C.A. Roulet, P. Favreau, V. Perret, G. Suarez, C. Hager Jörin, J. Goyette Pernot, D. Licina, Indoor air quality in Swiss primary schools: impacts of mechanical ventilation and seasonal variation, Build. Environ. 280 (2025) 113146, https://doi.org/10.1016/j.buildenv.2025.113146.

[4] I. Garbarienė, J. Pauraitė, D. Pashneva, A. Minderytė, K. Sarka, V. Dudoitis, L. Davulienė, M. Gaspariūnas, V. Kovalevskij, D. Lingis, L. Bučinskas, J. Šapolaitė, Ž. Ežerinskis, G. Mainelis, J. Ovadnevaitė, S. Kecorius, K. Plauškaitė-Šukienė, S. Byčenkienė, Indoor-outdoor relationship of submicron particulate matter in mechanically ventilated building: chemical composition, sources and infiltration factor, Build. Environ. 222 (2022) 109429, https://doi.org/10.1016/j.buildenv.2022.109429.

[5] I. Cunha-Lopes, V. Martins, T. Faria, C. Correia, S.M. Almeida, Children's exposure to sized-fractioned particulate matter and black carbon in an urban environment, Build. Environ. 155 (2019) 187–194, https://doi.org/10.1016/j.buildenv.2019.03.045.

[6] J. Madureira, I. Paciência, J. Rufo, M. Severo, E. Ramos, H. Barros, E. de Oliveira Fernandes, Source apportionment of CO_2, PM_{10} and VOCs levels and health risk assessment in naturally ventilated primary schools in Porto, Portugal, Build. Environ. 96 (2016) 198–205, https://doi.org/10.1016/j.buildenv.2015.11.031.

[7] B. Cabovská, G. Bekö, D. Teli, L. Ekberg, J.O. Dalenbäck, P. Wargocki, T. Psomas, S. Langer, Ventilation strategies and indoor air quality in Swedish primary school classrooms, Build. Environ. 226 (2022) 109744, https://doi.org/10.1016/j.buildenv.2022.109744.

[8] A. Zwoździak, I. Sówka, A. Worobiec, J. Zwoździak, A. Nych, The contribution of outdoor particulate matter (PM_1, $PM_{2.5}$, PM_{10}) to school indoor environment, Indoor and Built Environ 24 (2015) 1038–1047, https://doi.org/10.1177/1420326X14534093.

[9] P.N. Pegas, T. Nunes, C.A. Alves, J.R. Silva, S.L.A. Vieira, A. Caseiro, C.A. Pio, Indoor and outdoor characterisation of organic and inorganic compounds in city centre and suburban elementary schools of Aveiro, Portugal, Atmos. Environ. 55 (2012) 80–89, https://doi.org/10.1016/j.atmosenv.2012.03.059.

[10] P. Kumar, S. Hama, R.A. Abbass, K.V. Abhijith, A. Tiwari, D. Grassie, C. Mitsakou, Environmental quality in sixty primary and secondary school classrooms in London, J. Build. Eng. 91 (2024) 109549, https://doi.org/10.1016/j.jobe.2024.109549.

[11] A. Marcon, G. Pesce, P. Girardi, P. Marchetti, G. Blengio, S. de Zolt Sappadina, S. Falcone, G. Frapporti, F. Predicatori, R. De Marco, Association between PM_{10} concentrations and school absences in proximity of a cement plant in northern Italy, Int. J. Hyg. Environ. Health 217 (2014) 386–391, https://doi.org/10.1016/j.ijheh.2013.07.016.

[12] L. Zhang, H. Morisaki, Y. Wei, Z. Li, L. Yang, Q. Zhou, X. Zhang, W. Xing, M. Hu, M. Shima, A. Toriba, K. Hayakawa, N. Tang, Characteristics of air pollutants inside and outside a primary school classroom in Beijing and respiratory health impact on children, Environ. Pollut. 255 (2019) 113147, https://doi.org/10.1016/j.envpol.2019.113147.

[13] V. Martins, T. Faria, E. Diapouli, M.I. Manousakas, K. Eleftheriadis, M. Viana, S. M. Almeida, Relationship between indoor and outdoor size-fractionated particulate matter in urban microenvironments: levels, chemical composition and sources, Environ. Res. 183 (2020) 109203, https://doi.org/10.1016/j.envres.2020.109203.

[14] S.M. Almeida, T. Faria, V. Martins, N. Canha, E. Diapouli, K. Eleftheriadis, M. I. Manousakas, Source apportionment of children daily exposure to particulate matter, Sci. Total Environ. 835 (2022) 155349, https://doi.org/10.1016/j.scitotenv.2022.155349.

[15] C. Gama, A. Monteiro, C. Pio, A.I. Miranda, J.M. Baldasano, O. Tchepel, Temporal patterns and trends of particulate matter over Portugal: a long-term analysis of background concentrations, Air Qual. Atmos. Health. 11 (2018) 397–407, https://doi.org/10.1007/s11869-018-0546-8.

[16] I. Charres, L. Furst, E.D. Vicente, M. Soares, C. Viegas, R. Cervantes, P. Pena, M. Cerqueira, M. Feliciano, C. Alves, School air quality and thermal comfort: a multi-pollutant seasonal assessment, J. Build. Eng. 113 (2025) 113997, https://doi.org/10.1016/j.jobe.2025.113997.

[17] Insituto Portugues do Mar e da Atmosfera (IPMA), Clima de Portugal continental, (n.d.). https://www.ipma.pt/pt/educativa/tempo.clima/#:~:text=O%20clima%20de%20Portugal%20Continental,e%20pouco%20quente%20(Csb). (accessed August 20, 2025).

[18] Instituto Portugues do Mar e da Atmosfera, Normais climatológicas 1991 - 2020, (n.d.). https://www.ipma.pt/pt/oclima/normais.clima/1991-2020/#702 (accessed August 20, 2025).

[19] C. Girotti, L. Fernando Kowalski, T. Silva, E. Correia, A.R. Prata Shimomura, F. Akira Kurokawa, A. Lopes, Air pollution dynamics: the role of meteorological factors in PM_{10} concentration patterns across urban areas, City Environ. Interac. 25 (2025) 100184, https://doi.org/10.1016/j.cacint.2024.100184.

[20] T. Marques, M.S. Matias, E.F. da Silva, N. Durães, C. Patinha, Temporal and spatial groundwater contamination assessment using geophysical and hydrochemical methods: the industrial chemical complex of Estarreja (portugal) case study, Applied Sciences (Switzerland) 11 (2021) 6732, https://doi.org/10.3390/app11156732.

[21] M.L. Figueiredo, A. Monteiro, M. Lopes, J. Ferreira, C. Borrego, Air quality assessment of Estarreja, an urban industrialized area, in a coastal region of Portugal, Environ. Monit. Assess. 185 (2013) 5847–5860, https://doi.org/10.1007/s10661-012-2989-y.

[22] F. Cavalli, M. Viana, K.E. Yttri, J. Genberg, J.P. Putaud, Toward a standardised thermal-optical protocol for measuring atmospheric organic and elemental carbon: the EUSAAR protocol, Atmos. Meas. Tech. 3 (2010) 79–89, https://doi.org/10.5194/amt-3-79-2010.

[23] M. Millán-Martínez, D. Sánchez-Rodas, A.M. Sánchez de la Campa, J. de la Rosa, Contribution of anthropogenic and natural sources in PM_{10} during North African dust events in Southern Europe, Environ. Pollut. 290 (2021) 118065, https://doi.org/10.1016/j.envpol.2021.118065.

[24] O. Ramírez, A.M. Sánchez de la Campa, F. Amato, R.A. Catacolí, N.Y. Rojas, J. de la Rosa, Chemical composition and source apportionment of PM_{10} at an urban background site in a high–altitude Latin American megacity (Bogota, Colombia), Environ. Pollut. 233 (2018) 142–155, https://doi.org/10.1016/j.envpol.2017.10.045.

[25] Y.A. Cipoli, C. Alves, M. Rapuano, M. Evtyugina, I.C. Rienda, N. Kováts, A. Vicente, F. Giardi, L. Furst, T. Nunes, M. Feliciano, Nighttime–daytime PM_{10} source apportionment and toxicity in a remoteness inland city of the Iberian Peninsula, Atmos. Environ. 303 (2023) 119771, https://doi.org/10.1016/j.atmosenv.2023.119771.

[26] K. Karar, A.K. Gupta, Source apportionment of PM_{10} at residential and industrial sites of an urban region of Kolkata, India, Atmos. Res. 84 (2007) 30–41, https://doi.org/10.1016/j.atmosres.2006.05.001.

[27] C.A. Belis, F. Karagulian, F. Amato, M. Almeida, P. Artaxo, D.C.S. Beddows, V. Bernardoni, M.C. Bove, S. Carbone, D. Cesari, D. Contini, E. Cuccia, E. Diapouli, K. Eleftheriadis, O. Favez, I. El Haddad, R.M. Harrison, S. Hellebust, J. Hovorka, E. Jang, H. Jorquera, T. Kammermeier, M. Karl, F. Lucarelli, D. Mooibroek, S. Nava, J.K. Nøjgaard, P. Paatero, M. Pandolfi, M.G. Perrone, J.E. Petit, A. Pietrodangelo, P. Pokorná, P. Prati, A.S.H. Prevot, U. Quass, X. Querol, D. Saraga, J. Sciare, A. Sfetsos, G. Valli, R. Vecchi, M. Vestenius, E. Yubero, P.

K. Hopke, A new methodology to assess the performance and uncertainty of source apportionment models II: the results of two European intercomparison exercises, Atmos. Environ. 123 (2015) 240–250, https://doi.org/10.1016/j.atmosenv.2015.10.068.
[28] S. Hellebust, A. Allanic, I.P. O'Connor, J.C. Wenger, J.R. Sodeau, The use of real-time monitoring data to evaluate major sources of airborne particulate matter, Atmos. Environ. 44 (2010) 1116–1125, https://doi.org/10.1016/j.atmosenv.2009.11.035.
[29] L. Naidja, H. Ali-Khodja, S. Khardi, F. Bencharif-Madani, A. Terrouche, K. Lokorai, M. Bouziane, A. Charron, Source apportionment of $PM_{2.5}$ and their associated metallic elements by positive matrix factorization at a traffic site in Constantine, Algeria, Air Qual. Atmos. Health. 15 (2022) 2137–2155, https://doi.org/10.1007/s11869-022-01241-9.
[30] C.A. Gamelas, N. Canha, A. Vicente, A. Silva, S. Borges, C. Alves, Z. Kertesz, S. M. Almeida, Source apportionment of $PM_{2.5}$ before and after COVID-19 lockdown in an urban-industrial area of the Lisbon metropolitan area, Portugal, Urban Clim. 49 (2023) 101446, https://doi.org/10.1016/j.uclim.2023.101446.
[31] C. Vornanen-Winqvist, K. Järvi, M.A. Andersson, C. Duchaine, V. Létourneau, O. Kedves, L. Kredics, R. Mikkola, J. Kurnitski, H. Salonen, Exposure to indoor air contaminants in school buildings with and without reported indoor air quality problems, Environ. Int. 141 (2020) 105781, https://doi.org/10.1016/j.envint.2020.105781.
[32] S. Zhou, X. Wang, Y. Yang, R. Wang, J. Liao, P. Zhang, L. Liu, Y. Zhao, Y. Deng, Distribution and source identification of polycyclic aromatic hydrocarbons (PAHs) with PCA-MLR and PMF methods in the topsoil of Chengdu at SW, China, Sci. Total Environ. 908 (2024) 168263, https://doi.org/10.1016/j.scitotenv.2023.168263.
[33] B. Han, K. Hong, D. Shin, H.J. Kim, Y.J. Kim, S.B. Kim, S. Kim, C.H. Hwang, K. C. Noh, Field tests of indoor air cleaners for removal of $pm_{2.5}$ and pm_{10} in elementary school classrooms in Seoul, Korea, Aerosol Air Qual Res 22 (2022) 210383, https://doi.org/10.4209/aaqr.210383.
[34] C.A. Alves, R.C. Urban, P.N. Pegas, T. Nunes, Indoor/outdoor relationships between PM_{10} and associated organic compounds in a primary school, Aerosol Air Qual. Res. 14 (2014) 86–98, https://doi.org/10.4209/aaqr.2013.04.0114.
[35] T. Faria, V. Martins, N. Canha, E. Diapouli, M. Manousakas, P. Fetfatzis, M.I. Gini, S.M. Almeida, Assessment of children's exposure to carbonaceous matter and to PM major and trace elements, Sci. Total Environ. 807 (2022) 151021, https://doi.org/10.1016/j.scitotenv.2021.151021.
[36] A.E. Wittig, S. Takahama, A.Y. Khlystov, S.N. Pandis, S. Hering, B. Kirby, C. Davidson, Semi-continuous $PM_{2.5}$ inorganic composition measurements during the Pittsburgh air quality study, Atmos. Environ. 38 (2004) 3201–3213, https://doi.org/10.1016/j.atmosenv.2004.03.002.
[37] C.A. Gamelas, N. Canha, A. Vicente, A. Silva, S. Borges, C. Alves, Z. Kertesz, S. M. Almeida, Source apportionment of $PM_{2.5}$ before and after COVID-19 lockdown in an urban-industrial area of the Lisbon metropolitan area, Portugal, Urban Clim. 49 (2023) 101446, https://doi.org/10.1016/j.uclim.2023.101446.
[38] N. Mohamad, M.T. Latif, M.F. Khan, Source apportionment and health risk assessment of PM_{10} in a naturally ventilated school in a tropical environment, Ecotoxicol. Environ. Saf. 124 (2016) 351–362, https://doi.org/10.1016/j.ecoenv.2015.11.002.
[39] J. Cardoso, S.M. Almeida, T. Nunes, M. Almeida-Silva, M. Cerqueira, C. Alves, F. Rocha, P. Chaves, M. Reis, P. Salvador, B. Artiñano, C. Pio, Source apportionment of atmospheric aerosol in a marine dusty environment by ionic/composition mass balance (IMB), Atmos. Chem. Phys. 18 (2018) 13215–13230, https://doi.org/10.5194/acp-18-13215-2018.
[40] M. Almeida-Silva, T. Faria, D. Saraga, T. Maggos, H.T. Wolterbeek, S.M. Almeida, Source apportionment of indoor PM_{10} in Elderly Care Centre, Environ. Sci. Pollut. Res. 23 (2016) 7814–7827, https://doi.org/10.1007/s11356-015-5937-x.
[41] C. Perrino, A. Pelliccioni, L. Tofful, S. Canepari, Indoor PM_{10} in university classrooms: chemical composition and source behaviour, Atmos. Environ. 287 (2022) 119260, https://doi.org/10.1016/j.atmosenv.2022.119260.
[42] Y. Li, L. He, D. Xie, A. Zhao, L. Wang, N.M. Kreisberg, J. Jayne, Y. Liu, Strong temperature influence and indiscernible ventilation effect on dynamics of some semivolatile organic compounds in the indoor air of an office, Environ. Int. 165 (2022) 107305, https://doi.org/10.1016/j.envint.2022.107305.
[43] N. Barmparesos, D. Saraga, S. Karavoltsos, T. Maggos, V.D. Assimakopoulos, A. Sakellari, K. Bairachtari, M.N. Assimakopoulos, Chemical composition and source apportionment of pm10 in a green-roof primary school building, Appl. Sci. 10 (2020) 8464, https://doi.org/10.3390/app10238464.
[44] C. Alves, E.D. Vicente, T. Nunes, Y. Cipoli, I. Charres, E. Yubero, N. Galindo, J. Ryšavý, A. Leitão, Elemental and carbonaceous composition of PM_{10} and its oxidative potential in schools in Luanda, Atmos. Environ. 364 (2026) 121640, https://doi.org/10.1016/j.atmosenv.2025.121640.
[45] M. Leppänen, S. Peräniemi, H. Koponen, O. Sippula, P. Pasanen, The effect of the shoeless course on particle concentrations and dust composition in schools, Sci. Total Environ. 710 (2020) 136272, https://doi.org/10.1016/j.scitotenv.2019.136272.
[46] S. Kang, G. Ren, T. Lee, Y. Jo, Correlation between carbonaceous materials and fine particulate matters in urban school classrooms, Environ. Eng. Res. 29 (2024) 230516, https://doi.org/10.4491/eer.2023.516.
[47] Y. Xiao, L. Wang, M. Yu, T. Shui, L. Liu, J. Liu, Characteristics of indoor/outdoor $PM_{2.5}$ and related carbonaceous species in a typical severely cold city in China during heating season, Build. Environ. 129 (2018) 54–64, https://doi.org/10.1016/j.buildenv.2017.12.007.
[48] I. Salma, P.T. Varga, A. Vasanits, A. Machon, Secondary organic carbon in different atmospheric environments of a continental region and seasons, Atmos. Res. 278 (2022) 106360, https://doi.org/10.1016/j.atmosres.2022.106360.
[49] C. Alves, M. Evtyugina, E. Vicente, A. Vicente, I.C. Rienda, A.S. de la Campa, M. Tomé, I. Duarte, $PM_{2.5}$ chemical composition and health risks by inhalation near a chemical complex, J. Environ. Sci. (China) 124 (2023) 860–874, https://doi.org/10.1016/j.jes.2022.02.013.
[50] H. Mörtenkötter, C. Heilmeier, T. de Riese, S. Fendt, H. Spliethoff, Temperature resolved release of inorganic compounds from biomass, Fuel 357 (2024) 129939, https://doi.org/10.1016/j.fuel.2023.129939.
[51] N. Amil, M.T. Latif, M.F. Khan, M. Mohamad, Seasonal variability of $PM_{2.5}$ composition and sources in the Klang Valley urban-industrial environment, Atmos. Chem. Phys. 16 (2016) 5357–5381, https://doi.org/10.5194/acp-16-5357-2016.
[52] The European Parliament, On ambient air quality and cleaner air for Europe, 2024. https://eur-lex.europa.eu/legal-content/EN/TXT/PDF/?uri=OJ:L_202402881 (accessed June 6, 2025).
[53] The European Parliament, On ambient air quality and cleaner air for Europe, 2008. https://eur-lex.europa.eu/eli/dir/2008/50/oj/eng (accessed February 13, 2025).
[54] K. Glojek, V.D.N. Thuy, S. Weber, G. Uzu, M. Manousakas, R. Elazzouzi, K. Džepina, S. Darfeuil, P. Ginot, J.L. Jaffrezo, Annual variation of source contributions to PM_{10} and oxidative potential in a mountainous area with traffic, biomass burning, cement-plant and biogenic influences, Environ. Int. 189 (2024) 108787, https://doi.org/10.1016/j.envint.2024.108787.
[55] F. Oduber, A.I. Calvo, A. Castro, C. Alves, C. Blanco-Alegre, D. Fernández-González, J. Barata, G. Calzolai, S. Nava, F. Lucarelli, T. Nunes, A. Rodríguez, A. M. Vega-Maray, R.M. Valencia-Barrera, R. Fraile, One-year study of airborne sugar compounds: cross-interpretation with other chemical species and meteorological conditions, Atmos. Res. 251 (2021) 105417, https://doi.org/10.1016/j.atmosres.2020.105417.
[56] Z. Lin, Y. Ji, Y. Lin, Y. Yang, Y. Gao, M. Wang, Y. Xiao, J. Zhao, Y. Feng, W. Yang, B. Wang, PM_{10} and $PM_{2.5}$ chemical source profiles of road dust over China: composition, spatio-temporal distribution, and source apportionment, Urban Clim 51 (2023) 101672, https://doi.org/10.1016/j.uclim.2023.101672.
[57] L. Han, X. Yang, P. Zhang, Q. Xiao, S. Cheng, H. Wang, J. Guo, A. Zheng, Temporal variations of urban re-suspended road dust characteristics and its vital contributions to airborne $PM_{2.5}/PM_{10}$ during a long period in Beijing, Environ. Pollut. 330 (2023) 121727, https://doi.org/10.1016/j.envpol.2023.121727.
[58] Z. Yuhe, Y. Guangfei, L. Xianneng, Indoor $PM_{2.5}$ concentrations and students' behavior in primary school classrooms, J. Clean. Prod. 318 (2021) 128460, https://doi.org/10.1016/j.jclepro.2021.128460.
[59] A. Carrion-Matta, C.M. Kang, J.M. Gaffin, M. Hauptman, W. Phipatanakul, P. Koutrakis, D.R. Gold, Classroom indoor $PM_{2.5}$ sources and exposures in inner-city schools, Environ. Int. 131 (2019) 104968, https://doi.org/10.1016/j.envint.2019.104968.
[60] E. Diapouli, M. Manousakas, S. Vratolis, V. Vasilatou, T. Maggos, D. Saraga, T. Grigoratos, G. Argyropoulos, D. Voutsa, C. Samara, K. Eleftheriadis, Evolution of air pollution source contributions over one decade, derived by PM_{10} and $PM_{2.5}$ source apportionment in two metropolitan urban areas in Greece, Atmos. Environ. 164 (2017) 416–430, https://doi.org/10.1016/j.atmosenv.2017.06.016.
[61] S.K. Grange, A. Fischer, C. Zellweger, A. Alastuey, X. Querol, J.L. Jaffrezo, S. Weber, G. Uzu, C. Hueglin, Switzerland's PM_{10} and $PM_{2.5}$ environmental increments show the importance of non-exhaust emissions, Atmos. Environ X. 12 (2021) 100145, https://doi.org/10.1016/j.aeaoa.2021.100145.
[62] D. Smołka-Danielowska, M. Jabłońska, Chemical and mineral composition of ashes from wood biomass combustion in domestic wood-fired furnaces, Int J. Environ. Sci Technol. 19 (2022) 5359–5372, https://doi.org/10.1007/s13762-021-03506-9.
[63] C. Yang, Y. Wu, L. Zhang, G. Sun, H. Yao, Z. Li, X. Bi, Q. Huang, X. Feng, Spatiotemporal distributions and source apportionment of $pm_{2.5}$-bound antimony in Beijing, China, J. Geophys. Res. Atmos. 127 (2022) e2021JD036401, https://doi.org/10.1029/2021JD036401.
[64] T.H. Nguyen, Q.V. Pham, T.P.M. Nguyen, V.T. Vu, T.H. Do, M.T. Hoang, N. Thu Thuy Thi, T.B. Minh, Distribution characteristics and ecological risks of heavy metals in bottom ash, fly ash, and particulate matter released from municipal solid waste incinerators in northern Vietnam, Environ. Geochem. Health. 45 (2023) 2579–2590, https://doi.org/10.1007/s10653-022-01335-4.
[65] D.P. O'Loughlin, M.J. Haugen, J. Day, A.S. Brown, E.C. Braysher, N. Molden, A. E. Willis, M. MacFarlane, A.M. Boies, Multi-element analysis of tyre rubber for metal tracers, Environ. Int. 178 (2023) 108047, https://doi.org/10.1016/j.envint.2023.108047.
[66] H.H. Yang, S.M. Arafath, K.T. Lee, Y.S. Hsieh, Y.Te Han, Chemical characteristics of filterable and condensable $PM_{2.5}$ emissions from industrial boilers with five different fuels, Fuel 232 (2018) 415–422, https://doi.org/10.1016/j.fuel.2018.05.080.
[67] Y. Tong, J. Gao, K. Wang, H. Jing, C. Wang, X. Zhang, J. Liu, T. Yue, X. Wang, Y. Xing, Highly-resolved spatial-temporal variations of air pollutants from Chinese industrial boilers, Environ. Pollut. 289 (2021) 117931, https://doi.org/10.1016/j.envpol.2021.117931.
[68] A. Charron, L. Polo-Rehn, J.L. Besombes, B. Golly, C. Buisson, H. Chanut, N. Marchand, G. Guillaud, J.L. Jaffrezo, Identification and quantification of particulate tracers of exhaust and non-exhaust vehicle emissions, Atmos. Chem. Phys. 19 (2019) 5187–5207, https://doi.org/10.5194/acp-19-5187-2019.
[69] Agency for Toxic Substances and Disease Registry (US), Toxicological profile for barium and barium compounds, (2007). https://www.ncbi.nlm.nih.gov/books/NBK598780/ (accessed August 20, 2025).
[70] S. Heo, D.Y. Kim, Y. Kwoun, T.J. Lee, Y.M. Jo, Characterization and source identification of fine dust in Seoul elementary school classrooms, J. Hazard. Mater. 414 (2021) 125531, https://doi.org/10.1016/j.jhazmat.2021.125531.
[71] P.E. Rasmussen, C. Levesque, M. Chénier, H.D. Gardner, Contribution of metals in resuspended dust to indoor and personal inhalation exposures: relationships

between PM_{10} and settled dust, Build. Environ. 143 (2018) 513–522, https://doi.org/10.1016/j.buildenv.2018.07.044.
[72] E. Franceschi, F. Locardi, Strontium, a new marker of the origin of gypsum in cultural heritage? J. Cult. Herit. 15 (2014) 522–527, https://doi.org/10.1016/j.culher.2013.10.010.
[73] F. Xie, Y. Su, Y. Tian, Y. Shi, X. Zhou, P. Wang, R. Yu, W. Wang, J. He, J. Xin, C. Lü, The shifting of secondary inorganic aerosol formation mechanisms during haze aggravation: the decisive role of aerosol liquid water, Atmos. Chem. Phys. 23 (2023) 2365–2378, https://doi.org/10.5194/acp-23-2365-2023.
[74] E. Tutsak, B. Alfoldy, M.M. Mahfouz, J.A. Al-Thani, O. Yigiterhan, I. Shahid, R. J. Isaifan, M. Koçak, Chemical composition of indoor and outdoor $PM_{2.5}$ in the eastern Arabian Peninsula, Environ. Sci. Pollut. Res. 31 (2024) 49589–49600, https://doi.org/10.1007/s11356-024-34482-5.
[75] L. Tofful, C. Perrino, S. Canepari, Comparison study between indoor and outdoor chemical composition of $PM_{2.5}$ in two Italian areas, Atmosphere (Basel) 11 (2020) 368, https://doi.org/10.3390/ATMOS11040368.
[76] M. Lazaridis, V. Aleksandropoulou, J.E. Hanssen, C. Dye, K. Eleftheriadis, E. Katsivela, Inorganic and carbonaceous components in indoor/outdoor particulate matter in two residential houses in Oslo, Norway, J. Air Waste Manage. Assoc. 58 (2008) 346–356, https://doi.org/10.3155/1047-3289.58.3.346.
[77] Z. Szoboszlai, Z. Kertész, Z. Szikszai, A. Angyal, E. Furu, Z. Török, L. Daróczi, Á. Z. Kiss, Identification and chemical characterization of particulate matter from wave soldering processes at a printed circuit board manufacturing company, J. Hazard. Mater. 203-204 (2012) 308–316, https://doi.org/10.1016/j.jhazmat.2011.12.030.
[78] M. Komárek, V. Ettler, V. Chrastný, M. Mihaljevič, Lead isotopes in environmental sciences: a review, Environ. Int. 34 (2008) 562–577, https://doi.org/10.1016/j.envint.2007.10.005.
[79] K.Hans Wedepohl, The composition of the continental crust, Geochim. Cosmochim. Acta. 59 (1995) 1217–1232, https://doi.org/10.1016/0016-7037(95)00038-2.
[80] F. Sánchez-Soberón, J. Rovira, J. Sierra, M. Mari, J.L. Domingo, M. Schuhmacher, Seasonal characterization and dosimetry-assisted risk assessment of indoor particulate matter ($PM_{10\text{-}2.5}$, $PM_{2.5\text{-}0.25}$, and $PM_{0.25}$) collected in different schools, Environ. Res. 175 (2019) 287–296, https://doi.org/10.1016/j.envres.2019.05.035.